

CERN-EP-2023-173
22 August 2023

Observation of $\Xi_b^0 \rightarrow \Xi_c^+ D_s^-$ and $\Xi_b^- \rightarrow \Xi_c^0 D_s^-$ decays

LHCb collaboration[†]

Abstract

The $\Xi_b^0 \rightarrow \Xi_c^+ D_s^-$ and $\Xi_b^- \rightarrow \Xi_c^0 D_s^-$ decays are observed for the first time using proton-proton collision data collected by the LHCb experiment at a centre-of-mass energy of $\sqrt{s} = 13$ TeV, corresponding to an integrated luminosity of 5.1 fb^{-1} . The relative branching fractions times the beauty-baryon production cross-sections are measured to be

$$\mathcal{R} \left(\frac{\Xi_b^0}{\Lambda_b^0} \right) \equiv \frac{\sigma(\Xi_b^0)}{\sigma(\Lambda_b^0)} \times \frac{\mathcal{B}(\Xi_b^0 \rightarrow \Xi_c^+ D_s^-)}{\mathcal{B}(\Lambda_b^0 \rightarrow \Lambda_c^+ D_s^-)} = (15.8 \pm 1.1 \pm 0.6 \pm 7.7)\%,$$

$$\mathcal{R} \left(\frac{\Xi_b^-}{\Lambda_b^0} \right) \equiv \frac{\sigma(\Xi_b^-)}{\sigma(\Lambda_b^0)} \times \frac{\mathcal{B}(\Xi_b^- \rightarrow \Xi_c^0 D_s^-)}{\mathcal{B}(\Lambda_b^0 \rightarrow \Lambda_c^+ D_s^-)} = (16.9 \pm 1.3 \pm 0.9 \pm 4.3)\%,$$

where the first uncertainties are statistical, the second systematic, and the third due to the uncertainties on the branching fractions of relevant charm-baryon decays. The masses of Ξ_b^0 and Ξ_b^- baryons are measured to be $m_{\Xi_b^0} = 5791.12 \pm 0.60 \pm 0.45 \pm 0.24 \text{ MeV}/c^2$ and $m_{\Xi_b^-} = 5797.02 \pm 0.63 \pm 0.49 \pm 0.29 \text{ MeV}/c^2$, where the uncertainties are statistical, systematic, and those due to charm-hadron masses, respectively.

Submitted to Eur. Phys. J. C

© 2023 CERN for the benefit of the LHCb collaboration. CC BY 4.0 licence.

[†]Authors are listed at the end of this paper.

1 Introduction

Hadrons are systems of quarks bound by the strong interaction, described at the fundamental level by quantum chromodynamics (QCD). The production and decay of hadrons involve the nonperturbative regime of QCD, making calculations challenging. Much progress has been made in recent years in experimental and theoretical studies of beauty mesons, with the aim of testing the Standard Model and searching for new physics through measurements of branching fractions, CP asymmetries and rare decays [1]. However, many aspects of beauty baryons are still largely unknown, due to the difficulties to produce and detect them in experiments other than those operating at the Large Hadron Collider.

So far, the Λ_b^0 baryon has been more widely studied than the other beauty baryons, including Ξ_b^0 and Ξ_b^- .¹ Very few decay modes have been measured for $\Xi_b^{0(-)}$ baryons [2]. According to the quark model, the three beauty baryons Λ_b^0 , Ξ_b^0 and Ξ_b^- (referred to as H_b in the following) form an $SU(3)$ flavour multiplet, as do the Λ_c^+ , Ξ_c^+ and Ξ_c^0 states (referred to as H_c in the following). The H_b decay is dominated by the weak transition of the b quark while the two light quarks serve as compact spectators [3,4]. According to heavy quark effective theory, the three decays of bottom baryons into two charm hadrons, $H_b \rightarrow H_c D_s^-$, should have approximately the same partial width [5,6]. The $\Lambda_b^0 \rightarrow \Lambda_c^+ D_s^-$ decay has been measured to have a branching fraction (\mathcal{B}) at the percent level [7], but no measurements for $\Xi_b^{0(-)} \rightarrow \Xi_c^{+(0)} D_s^-$ decays are available. Measurements of these decays not only test the $SU(3)$ symmetry but also give insights into the dynamics of beauty-baryon weak decays.

Beauty baryons of all species are abundantly produced at the LHC [8–11], allowing them to be intensively studied. This analysis presents the first observation of $\Xi_b^0 \rightarrow \Xi_c^+ D_s^-$ and $\Xi_b^- \rightarrow \Xi_c^0 D_s^-$ decays, using data from proton-proton (pp) collisions at a centre-of-mass energy of $\sqrt{s} = 13$ TeV collected by LHCb detector and corresponding to an integrated luminosity of 5.1 fb^{-1} . The relative production rates of the decays, \mathcal{R} , defined to be

$$\mathcal{R} \left(\frac{\Xi_b^0}{\Lambda_b^0} \right) \equiv \frac{\sigma(\Xi_b^0)}{\sigma(\Lambda_b^0)} \times \frac{\mathcal{B}(\Xi_b^0 \rightarrow \Xi_c^+ D_s^-)}{\mathcal{B}(\Lambda_b^0 \rightarrow \Lambda_c^+ D_s^-)}, \quad (1)$$

$$\mathcal{R} \left(\frac{\Xi_b^-}{\Lambda_b^0} \right) \equiv \frac{\sigma(\Xi_b^-)}{\sigma(\Lambda_b^0)} \times \frac{\mathcal{B}(\Xi_b^- \rightarrow \Xi_c^0 D_s^-)}{\mathcal{B}(\Lambda_b^0 \rightarrow \Lambda_c^+ D_s^-)}, \quad (2)$$

$$\mathcal{R} \left(\frac{\Xi_b^0}{\Xi_b^-} \right) \equiv \frac{\sigma(\Xi_b^0)}{\sigma(\Xi_b^-)} \times \frac{\mathcal{B}(\Xi_b^0 \rightarrow \Xi_c^+ D_s^-)}{\mathcal{B}(\Xi_b^- \rightarrow \Xi_c^0 D_s^-)}, \quad (3)$$

are measured, where σ denotes the production cross-section. Given the similar lifetimes of the three beauty baryons [2], if the decay widths of the three beauty-baryon decays are also similar, the variables defined in Eq. 1- 3 provide measurements of the H_b production cross-section ratios, *i.e.* b -quark fragmentation fraction ratios. Isospin symmetry assures that $\sigma(\Xi_b^0)/\sigma(\Xi_b^-) \approx 1$ to a good approximation, resulting in $\mathcal{R} \left(\frac{\Xi_b^0}{\Xi_b^-} \right) \approx 1$ at leading order, which is tested in this analysis. The masses of the Ξ_b^0 and Ξ_b^- baryons and the mass differences between the three beauty baryons are also measured.

¹The inclusion of charge-conjugate processes is implied throughout.

2 Detector, samples and analysis strategy

The LHCb detector [12,13] is a single-arm forward spectrometer covering the pseudorapidity range $2 < \eta < 5$, designed for the study of particles containing b or c quarks. The detector includes a high-precision tracking system consisting of a silicon-strip vertex detector surrounding the pp interaction region, a large-area silicon-strip detector located upstream of a dipole magnet with a bending power of about 4 Tm, and three stations of silicon-strip detectors and straw drift tubes placed downstream of the magnet. The tracking system provides a measurement of the momentum, p , of charged particles with a relative uncertainty that varies from 0.5% at low momentum to 1.0% at 200 GeV/ c . The momentum scale is calibrated using samples of $J/\psi \rightarrow \mu^+\mu^-$ and $B^+ \rightarrow J/\psi K^+$ decays collected concurrently with the data samples used for this analysis [14,15]. The relative uncertainty of this procedure is determined to be 3×10^{-4} using samples of other fully reconstructed B , Υ , and K_S^0 -meson decays. The minimum distance of a track to a primary pp collision vertex (PV), the impact parameter (IP), is measured with a resolution of $(15 + 29/p_T) \mu\text{m}$, where p_T is the component of the momentum transverse to the beam, in GeV/ c . Different types of charged hadrons are distinguished using information from two ring-imaging Cherenkov detectors. Photons, electrons and hadrons are identified by a calorimeter system consisting of scintillating-pad and preshower detectors, an electromagnetic and a hadronic calorimeter.

The data used in this analysis come from pp collisions at $\sqrt{s} = 13 \text{ TeV}$, collected by LHCb between 2016 and 2018. The total integrated luminosity is 5.1 fb^{-1} . The online event selection of LHCb is performed by a trigger [16], which consists of a hardware stage, based on information from the calorimeter and muon systems, followed by a software stage, which applies a full event reconstruction. At the hardware trigger stage, events are required to have a muon with high p_T or a hadron, photon or electron with high transverse energy in the calorimeters. A global hardware trigger decision is required based on the reconstructed candidate, the rest of the event, or a combination of both. The software trigger requires a two-, three- or four-track secondary vertex with a significant displacement from any primary pp interaction vertex. At least one charged particle within the secondary vertex must have a transverse momentum $p_T > 1.6 \text{ GeV}/c$ and be inconsistent with originating from any PV.

Simulated decays are used to perform event selections, calculate reconstruction and selection efficiencies, and determine the invariant-mass distributions of the reconstructed signal H_b candidates. In the simulation, pp collisions are generated using PYTHIA 8 [17] with a specific LHCb configuration [13]. Decays of unstable particles are described by EVTGEN [18], in which final-state radiation is generated using PHOTOS [19]. The interaction of the generated particles with the detector, and its response, are simulated using the GEANT4 [20] toolkit as described in Ref. [21].

The Λ_c^+ and Ξ_c^+ baryons are reconstructed in the $pK^-\pi^+$ final state, and the Ξ_c^0 baryon in the $pK^-K^-\pi^+$ final state. The D_s^- mesons are reconstructed by combining three charged particles identified as K^- , K^+ and π^- mesons. The H_c candidates are combined with D_s^- candidates to form the H_b candidates. The three \mathcal{R} parameters are

Table 1: Branching fractions of H_c decays [2].

Decay	Branching fraction
$\Lambda_c^+ \rightarrow pK^-\pi^+$	$(6.28 \pm 0.32) \times 10^{-2}$
$\Xi_c^+ \rightarrow pK^-\pi^+$	$(6.2 \pm 3.0) \times 10^{-3}$
$\Xi_c^0 \rightarrow pK^-K^-\pi^+$	$(4.8 \pm 1.2) \times 10^{-3}$

76 defined according to

$$\mathcal{R} \left(\frac{\Xi_b^0}{\Lambda_b^0} \right) = \frac{N(\Xi_b^0 \rightarrow \Xi_c^+ D_s^-) / \varepsilon(\Xi_b^0 \rightarrow \Xi_c^+ D_s^-)}{N(\Lambda_b^0 \rightarrow \Lambda_c^+ D_s^-) / \varepsilon(\Lambda_b^0 \rightarrow \Lambda_c^+ D_s^-)} \times \frac{\mathcal{B}(\Lambda_c^+ \rightarrow pK^-\pi^+)}{\mathcal{B}(\Xi_c^+ \rightarrow pK^-\pi^+)}, \quad (4)$$

$$\mathcal{R} \left(\frac{\Xi_b^-}{\Lambda_b^0} \right) = \frac{N(\Xi_b^- \rightarrow \Xi_c^0 D_s^-) / \varepsilon(\Xi_b^- \rightarrow \Xi_c^0 D_s^-)}{N(\Lambda_b^0 \rightarrow \Lambda_c^+ D_s^-) / \varepsilon(\Lambda_b^0 \rightarrow \Lambda_c^+ D_s^-)} \times \frac{\mathcal{B}(\Lambda_c^+ \rightarrow pK^-\pi^+)}{\mathcal{B}(\Xi_c^0 \rightarrow pK^-K^-\pi^+)}, \quad (5)$$

$$\mathcal{R} \left(\frac{\Xi_b^0}{\Xi_b^-} \right) = \frac{N(\Xi_b^0 \rightarrow \Xi_c^+ D_s^-) / \varepsilon(\Xi_b^0 \rightarrow \Xi_c^+ D_s^-)}{N(\Xi_b^- \rightarrow \Xi_c^0 D_s^-) / \varepsilon(\Xi_b^- \rightarrow \Xi_c^0 D_s^-)} \times \frac{\mathcal{B}(\Xi_c^0 \rightarrow pK^-K^-\pi^+)}{\mathcal{B}(\Xi_c^+ \rightarrow pK^-\pi^+)}, \quad (6)$$

77 where N , ε , and \mathcal{B} denote the observed signal yields, the total experimental efficiencies,
78 and the branching fractions, respectively. The world averages of branching fractions of
79 corresponding H_c decays [2] are summarised in Table 1. The signal yields are determined
80 using unbinned extended maximum-likelihood fits of the $H_c D_s^-$ invariant-mass distributions.
81 The efficiencies are determined using simulated signal decays, calibrated by data driven
82 methods.

83 3 Event selections and efficiencies

84 In order to suppress background due to random combinations of either the H_c or D_s^- , and
85 misidentification of final-state particles, a series of event selections are performed. Firstly,
86 all final-state particles are required to be separated from any PV and have $p_T > 100$ MeV/ c .
87 They must also be correctly identified, with a high significance, as either a proton, kaon or
88 pion, using combined information from the tracking system and sub-detectors related to
89 particle identification (PID) [12, 22]. The final states of the H_c and D_s^- candidates must
90 have a scalar sum of $p_T > 1.8$ GeV/ c , and at least one of them must have $p_T > 0.5$ GeV/ c
91 and $p > 5$ GeV/ c . They are additionally required to form a good vertex that is significantly
92 separated from any PV. The H_c and D_s^- candidates should have an invariant mass within
93 ± 25 MeV/ c^2 of the previous world average mass value [2], and their vertices should be
94 consistent with being downstream of the H_b vertex. The H_b candidate formed by the
95 H_c and D_s^- hadrons must have a good vertex separated from its associated PV, and its
96 momentum must point back to the associated PV. The final-state particles of the H_b must
97 have a scalar sum of $p_T > 5$ GeV/ c . Finally, H_b candidates with transverse momentum
98 $p_T > 4$ GeV and rapidity $2.5 < y < 4$ are retained for further analysis.

99 There are backgrounds due to genuine particle decays, where a pion or kaon decay
100 product is misidentified as a proton, resulting in a H_c candidate. For Λ_c^+ and Ξ_c^+ candidates,
101 they include $\phi \rightarrow K^+K^-$, $D_s^+ \rightarrow K^+K^-\pi^+$, $D^+ \rightarrow K^+K^-\pi^+$ and $D^0 \rightarrow K^+K^-$ decays
102 with the K^+ meson misidentified as a proton, and $D^+ \rightarrow K^-\pi^+\pi^+$, $D^0 \rightarrow K^-\pi^+$ decays
103 with the π^+ meson misidentified as a proton. For Ξ_c^0 candidates, there are backgrounds
104 due to $\phi \rightarrow K^+K^-$ and $D^0 \rightarrow K^+K^-K^-\pi^+$ decays with the K^+ meson misidentified as a

105 proton. For D_s^- candidates, the $\Lambda_c^+ \rightarrow pK^-\pi^+$ background with the proton misidentified
 106 as a K^+ meson is considered. To remove these background, candidates are required
 107 to satisfy strict PID requirements or their invariant masses, calculated with alternative
 108 mass hypotheses for final states, must be outside a region around the known mass of
 109 the corresponding genuine particle (ϕ , D_s^+ , D^+ , D^0 , or Λ_c^+) [2]. Backgrounds due to
 110 $D^- \rightarrow K^+\pi^-\pi^-$ decays are also considered, and are found to be negligible.

111 Further event selections are performed using a gradient-boosted decision tree
 112 (BDTG) [23] algorithm to reduce combinatorial backgrounds. Due to the similarity
 113 between the topologies of the three $H_b \rightarrow H_c D_s^-$ decays, and to benefit from a cancellation
 114 of systematic uncertainties related to the BDTG selection in the \mathcal{R} measurements, the
 115 BDTG classifier is trained with the Ξ_b^0 samples and is applied to all the three decay modes.
 116 The BDTG algorithm is trained to distinguish simulated $\Xi_b^0 \rightarrow \Xi_c^+ D_s^-$ decays from the
 117 candidates in the high mass sideband ($m(\Xi_b^0) > 5950 \text{ MeV}/c^2$) of data, which are repre-
 118 sentative of the background. The BDTG classifier combines seventeen variables, including
 119 kinematic, topological and PID information, to get a single discriminating response. The
 120 optimal requirement on the BDTG response is determined by maximising the figure of
 121 merit $F \equiv S/\sqrt{S+B}$, where S (B) is the expected number of signal (background) yield in
 122 the signal region of data with BDTG response greater than a given value. The signal region
 123 is defined to be $\pm 30 \text{ MeV}/c^2$ around the previous world average of H_b mass [2], which is
 124 about three times the experimental resolution. The value of S is calculated as the product
 125 of the BDTG efficiency for the signal and the signal yield before the BDTG requirement,
 126 which is obtained by fitting to Ξ_b^0 invariant-mass distribution in data. Similarly, B is
 127 calculated as the background retention rate multiplied by the estimated background in the
 128 signal region without the BDTG requirement. The background retention rate is evaluated
 129 with the data in the high-mass sideband data, and the number of background candidates
 130 in the signal region is estimated with a fit to Ξ_b^0 invariant-mass distribution in the high
 131 invariant-mass sideband region of the data, with a subsequent extrapolation to the signal
 132 mass region. The optimal BDTG requirement corresponds to a signal efficiency of about
 133 95% with respect to other selection requirements for all three H_b decay modes.

134 The total efficiency is calculated as the product of efficiencies of detector acceptance,
 135 reconstruction, and selection. It is estimated using the simulated signal decays. These
 136 samples are calibrated such that the shapes of several key distributions match those
 137 of the data: the PID response, H_b kinematics, total charged-track multiplicity and H_c
 138 resonant structures. The $D_s^- \rightarrow K^+K^-\pi^-$ decay is simulated using measured Dalitz
 139 compositions [24], thus no corrections are applied. The PID efficiencies for the different
 140 particle species are measured using charm hadron samples in data [22]. The large sample of
 141 $\Lambda_b^0 \rightarrow \Lambda_c^+ D_s^-$ decays is used to correct for the transverse momentum, pseudorapidity, and
 142 charged-track multiplicity distributions of the three H_b decay modes. Further corrections
 143 are made to align the shapes of the charged-track multiplicity distributions in the data
 144 and simulation for Ξ_b decays. The H_c Dalitz distribution is compared between the data
 145 and simulation; a weight-based correction is applied to improve the agreement. The
 146 track-finding efficiency in simulation is found to be slightly different from that in data, and
 147 this difference is corrected as a function of the momentum and pseudorapidity of final-state
 148 particles [25]. The correction factors are generally obtained in bins of relevant variables
 149 apart from that for the Ξ_c^0 Dalitz distribution, where the large number of dimensions
 150 implies a limited number of candidates per bin. An unbinned multivariate algorithm
 151 is therefore used [26]. The ratios of efficiencies between Λ_b^0 , Ξ_b^0 , and Ξ_b^- decays are

152 determined to be

$$\begin{aligned}\frac{\varepsilon(\Xi_b^0)}{\varepsilon(\Lambda_b^0)} &= 1.101 \pm 0.010, \\ \frac{\varepsilon(\Xi_b^-)}{\varepsilon(\Lambda_b^0)} &= 0.515 \pm 0.005, \\ \frac{\varepsilon(\Xi_b^0)}{\varepsilon(\Xi_b^-)} &= 2.138 \pm 0.017,\end{aligned}$$

153 where the uncertainties are statistical only. The Λ_b^0 and Ξ_b^0 decays have a similar efficiency,
154 while the smaller Ξ_b^- efficiency is due to one more final-state particle.

155 4 Signal yield determination and mass measurements

156 To obtain the yields of signal H_b decays, an extended maximum likelihood fit is performed
157 to the Λ_b^0 , Ξ_b^0 , and Ξ_b^- invariant-mass spectra. A kinematic refit [27] is applied to the
158 H_b decays to improve the mass resolution, constraining the D_s^- and H_c masses to their
159 previously measured values [2] and the H_b momentum to point back to its PV. The fitted
160 mass region is $5450 - 5800 \text{ MeV}/c^2$, $5600 - 6100 \text{ MeV}/c^2$, and $5600 - 6000 \text{ MeV}/c^2$ for the
161 Λ_b^0 , Ξ_b^0 , and Ξ_b^- decays, respectively.

162 As shown in Fig. 1, three components are identified in each H_b mass spectrum. The
163 signal component is parameterised using the sum of a Gaussian and a double-sided Crystal
164 Ball function (DSCB) [28] sharing a common mean. The common mean and the average
165 resolution of the Gaussian and the DSCB distribution are parameters that vary freely in
166 the fit, while the other parameters have values fixed to those obtained from simulation.
167 The contribution of combinatorial backgrounds in the mass spectrum is modelled using
168 a second order polynomial, with all parameters varying freely. The peaking structure
169 in the low invariant-mass region corresponds to partially reconstructed $H_b \rightarrow H_c D_s^- X$
170 decays where X is an undetected particle. Distributions from data in the low mass region
171 are found to be consistent with the $H_b \rightarrow H_c D_s^{*-}$, $D_s^{*-} \rightarrow D_s^- \gamma$ sequential decay, where
172 the γ is not reconstructed. The subsequent $H_c D_s^-$ invariant-mass distribution depends
173 on the D_s^{*-} helicity projection, for which three possibilities, helicities of ± 1 and 0, are
174 allowed. The mass distributions for helicities of $+1$ and -1 are identical. Samples are
175 generated with helicities of 1 and 0, and corresponding $H_c D_s^-$ invariant-mass distributions
176 are obtained. The distributions convoluted with experimental resolutions are used to fit
177 data. The fraction of the component with a helicity of 0 varies freely in the fit.

178 Figure 1 shows the H_b invariant-mass distributions superimposed by the fit re-
179 sults. The signal yields for Λ_b^0 , Ξ_b^0 and Ξ_b^- decays are $(2.609 \pm 0.017) \times 10^4$,
180 462 ± 29 , and 175 ± 14 , respectively. The masses for Λ_b^0 , Ξ_b^0 and Ξ_b^- baryons
181 are measured to be $m_{\Lambda_b^0} = 5619.34 \pm 0.06 \text{ MeV}/c^2$, $m_{\Xi_b^0} = 5791.12 \pm 0.60 \text{ MeV}/c^2$, and
182 $m_{\Xi_b^-} = 5797.02 \pm 0.63 \text{ MeV}/c^2$, respectively, where the uncertainties are statistical only.

183 4.1 Non-dicharm background

184 The sample of $H_b \rightarrow H_c D_s$ decays is polluted by decays with a single charm hadron
185 (one-charm) or charmless decays that have the same final-state particles but without the

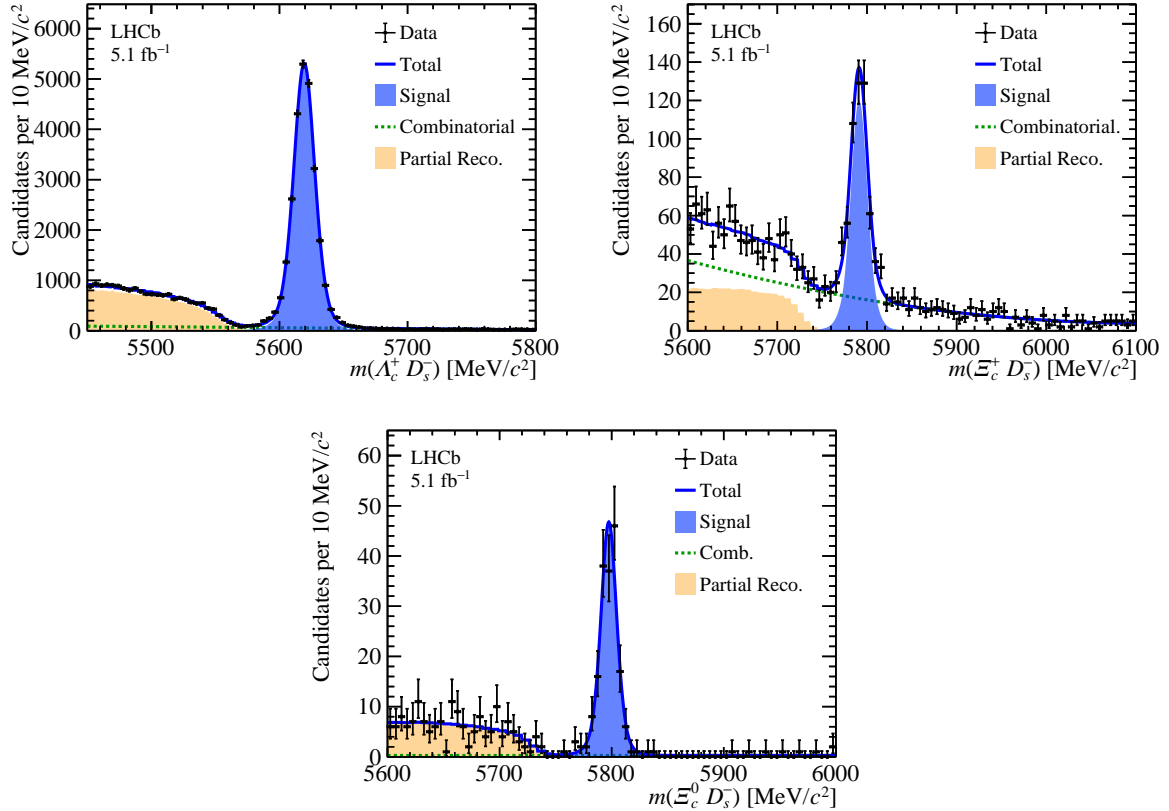


Figure 1: Invariant-mass distributions of (top left) Λ_b^0 , (top right) Ξ_b^0 , and (bottom) Ξ_b^- decays. The data are overlaid on the fit results.

186 intermediate H_c or D_s^- hadron, referred to as non-dicharm decays. For these peaking
 187 background contributions, their H_b invariant-mass distributions are signal-like, but the
 188 H_c or D_s^- invariant-mass distributions are flat. The distributions of non-dicharm compo-
 189 nents in the H_c or D_s^- invariant-mass distribution are found to be approximately linear.
 190 Therefore, the H_b signal yields in the H_c and D_s^- sideband regions are extrapolated to
 191 the signal region (± 25 MeV/ c^2 around the previously measured H_c and D_s^- masses [2]) to
 192 estimate the contamination of non-dicharm background in the signal region. Details of the
 193 estimation are shown in Appendix A. The fractions of non-dicharm decays are measured
 194 to be $(5.70 \pm 0.13)\%$, $(8.39 \pm 1.75)\%$ and $(6.44 \pm 1.48)\%$ for Λ_b^0 , Ξ_b^0 and Ξ_b^- decays, respec-
 195 tively. These background contributions are subtracted from the total signal yield obtained
 196 from the fit. The non-dicharm contamination is dominated by the $H_b \rightarrow H_c(K^+K^-\pi^-)$
 197 component.

198 5 Systematic uncertainties

199 5.1 Uncertainties on the branching fraction

200 Measurements of the ratios of branching fractions are affected by a number of systematic
 201 uncertainties. Apart from those due to the input charm-decay branching fractions, they are
 202 generally related to either the signal yields or the efficiencies. Due to the similar topologies

203 of the three H_b decays, many sources of systematic uncertainties are either cancelled
 204 or largely suppressed in ratios of the branching fractions. The remaining systematic
 205 uncertainties are outlined below and summarised in Table 2.

206 5.1.1 Systematic uncertainties on the signal yield

207 The fit results are affected by the imperfect modelling of the signal, the combinatorial
 208 background and the partially reconstructed background. Variations of the signal model
 209 are studied by modifying the fixed parameters that are obtained from simulation. For the
 210 background modelling, a polynomial of third order is used instead of one of second order.
 211 In order to study the impact of the modelling of the partially reconstructed background in
 212 the signal yield, the lower edge of the fit range is increased to 5575, 5740, and 5750 MeV/ c^2
 213 for the Λ_b^0 , Ξ_b^0 , and Ξ_b^- decay modes, respectively, excluding partially reconstructed
 214 background. Alternative fits to data with these alternate approaches are performed. The
 215 largest deviation of the H_b signal yield in these alternative fits from the nominal result
 216 is taken as the systematic uncertainty on the signal yield due to the modelling of the fit
 217 components, which is at the level of 2%.

218 The uncertainty on the fraction of non-dicharm background discussed in Section 4.1
 219 originates from the limited size of the data sample and possible nonlinearity of the H_c and
 220 D_s^- background invariant-mass distributions. The effect is studied by using alternative
 221 regions of sideband data to calculate the non-dicharm yield, and the difference with respect
 222 to the nominal results is quoted as the systematic uncertainty, which is found to be at the
 223 subpercent level.

224 5.1.2 Systematic uncertainties on the efficiency

225 As efficiencies are studied using simulation samples, the systematic uncertainty on efficien-
 226 cies arises due to the limited size of simulation samples and imperfect simulations. The
 227 uncertainty due to the limited simulation sample size is 1.0% for the three H_b efficiency
 228 ratios.

229 The hardware trigger is approximately modeled in the simulation. The trigger efficiency
 230 is measured in the data [29], and the difference between data and simulation is assigned
 231 as a systematic uncertainty. This systematic uncertainty is found to be approximately
 232 cancelled among the three H_b decay modes, resulting in a relative difference of less than
 233 1.5% between data and simulation on the efficiency ratios of the two H_b decay modes. A
 234 common value of 1.5% is quoted as the relative systematic uncertainty of the hardware
 235 trigger on the relative branching fraction.

236 The estimation of the reconstruction efficiency is affected by the model of detector
 237 material in simulation which affects the description of interaction between the final-state
 238 particles and the material. It leads to a relative uncertainty of 1.2% between Ξ_b^- and
 239 the other two H_b decays due to one additional kaon in the Ξ_b^- decay [30]. Moreover, the
 240 estimation of the track-finding efficiency in data and simulation is subjected to uncertainties
 241 related to the detector occupancy and limited sizes of the calibration samples [25]. The
 242 former gives a relative value of 0.8% per track, while the latter results in an uncertainty of
 243 around 0.1% on the efficiency ratios. In total the uncertainty on the ratio of reconstruction
 244 efficiency is about 1.6% between Ξ_b^- and Λ_b^0 decays, and between Ξ_b^0 and Ξ_b^- decays. It
 245 is below 0.1% for the efficiency ratio between Ξ_b^0 and Λ_b^0 decays.

Table 2: Systematic uncertainties on the relative branching fraction measurements. Results are given as relative uncertainties.

Source	$\mathcal{R}\left(\frac{\Xi_b^0}{\Lambda_b^0}\right)$	$\mathcal{R}\left(\frac{\Xi_b^-}{\Lambda_b^0}\right)$	$\mathcal{R}\left(\frac{\Xi_b^0}{\Xi_b^-}\right)$
Imperfect modelling of invariant-mass fit	2.7%	1.3%	3.4%
Fraction of non-dicharm background	2.0%	1.6%	2.5%
Limited simulation sample size	0.9%	1.0%	0.8%
Trigger efficiency	1.5%	1.5%	1.5%
Reconstruction efficiency	0.1%	1.6%	1.7%
Corrections to simulations	1.3%	4.3%	4.3%
Total	3.8%	5.4%	6.5%

246 Corrections to simulation samples to match data to the distributions of final-state
 247 particle PID responses, H_b kinematics, charged-track multiplicity and H_c Dalitz distri-
 248 butions are subject to uncertainties. Uncertainties on the corrections of PID responses
 249 are evaluated using alternative corrections and measuring the relative change of efficien-
 250 cies [22], which is found to be negligible. The uncertainty on corrections of H_b kinematics
 251 is studied with pseudoexperiments. For each pseudoexperiment, the correction factor in
 252 each transverse momentum and rapidity of the H_b baryon is varied following a Gaussian
 253 distribution constructed from the nominal value and its uncertainty. The new correction
 254 factors are used to calculate the efficiency. The width of the efficiency distribution among
 255 a set of pseudoexperiments is taken as the systematic uncertainty. Similar studies are
 256 performed for corrections of the charge-track multiplicity and Λ_c^+ , Ξ_c^+ Dalitz distributions.
 257 The uncertainty of the unbinned correction to the Ξ_c^0 Dalitz distribution is studied by
 258 varying the configurations of the algorithm [26]. In total the uncertainty on the efficiency
 259 ratio originating from corrections to simulation samples is about 4.3% between Ξ_b^- and
 260 Λ_b^0 , 4.3% between Ξ_b^0 and Ξ_b^- , and 1.3% between Ξ_b^0 and Λ_b^0 .

261 5.2 Uncertainties on the H_b mass measurements

262 The uncertainties on the mass and mass difference measurements come from the invariant-
 263 mass fit model, the momentum scale calibration, and the uncertainties on the Ξ_c and D_s^-
 264 masses [2]. They are summarised in Table 3 and Table 4.

265 The H_b mass determined from the fit to the invariant-mass distribution is affected by
 266 the imperfect modelling of the signal, the combinatorial background and the partially
 267 reconstructed background. Variations of the model for each fit component are studied in
 268 the same way as for the determination of the uncertainties on the signal yield described in
 269 Sec. 5.1.1. The largest variation of the mass obtained in these alternative fits compared
 270 to the nominal one is considered as the systematic uncertainty, which is 0.02, 0.19 and
 271 0.09 MeV/ c^2 for $m_{\Lambda_b^0}$, $m_{\Xi_b^0}$ and $m_{\Xi_b^-}$, respectively. The larger uncertainty for $m_{\Xi_b^0}$ is due
 272 to the higher background level.

273 Due to effects such as an imperfect alignment of the tracking system and the uncertainty
 274 on the magnetic field, the measured track momenta need to be calibrated to correct for
 275 possible biases. The calibration is performed using the masses of known hadrons [31, 32]
 276 with a precision of 0.03%. The uncertainty is propagated to the H_b mass measurement

Table 3: Systematic uncertainties for the H_b mass measurements.

Source	$m_{\Lambda_b^0}$ [MeV/ c^2]	$m_{\Xi_b^0}$ [MeV/ c^2]	$m_{\Xi_b^-}$ [MeV/ c^2]
Mass fit model	0.02	0.19	0.09
Momentum scale calibration	0.44	0.41	0.48
Uncertainties on the H_c and D_s^- masses	0.16	0.24	0.29

Table 4: Systematic uncertainties for the H_b mass-difference measurements.

Source	$m_{\Xi_b^0} - m_{\Lambda_b^0}$ [MeV/ c^2]	$m_{\Xi_b^-} - m_{\Lambda_b^0}$ [MeV/ c^2]	$m_{\Xi_b^-} - m_{\Xi_b^0}$ [MeV/ c^2]
Mass fit model	0.19	0.09	0.21
Momentum scale calibration	0.03	0.04	0.07
Uncertainties on the H_c mass	0.27	0.31	0.23

by varying the calibration by ± 1 standard deviation. Half of the difference between the two corresponding new H_b masses is taken as the systematic uncertainty. The result, about $0.4 \text{ MeV}/c^2$, approximately scales with the energy release of the decay as $(m(H_b) - m(H_c) - m(D_s^-)) \times 0.03\%$. The uncertainty due to momentum scale calibration is assumed to be fully correlated for the three H_b masses.

As mentioned in Sec. 4, the H_b invariant mass is calculated with the D_s^- and H_c masses constrained to their previous world averages [2]. The systematic uncertainty due to the H_c and D_s^- masses is 0.16, 0.24, and 0.29 MeV/c^2 for the Λ_b^0 , Ξ_b^0 , and Ξ_b^- mass measurement, respectively. When measuring the mass difference between two different H_b states, the uncertainty on the D_s^- mass is cancelled. The remaining uncertainty on the H_c mass varies between 0.23 and 0.31 MeV/c^2 depending on mass difference.

6 Results

Using the results presented in the previous sections, the H_b masses and mass differences are measured to be

$$\begin{aligned}
 m_{\Lambda_b^0} &= 5619.34 \pm 0.06 \pm 0.44 \pm 0.16 \text{ MeV}/c^2, \\
 m_{\Xi_b^0} &= 5791.12 \pm 0.60 \pm 0.45 \pm 0.24 \text{ MeV}/c^2, \\
 m_{\Xi_b^-} &= 5797.02 \pm 0.63 \pm 0.49 \pm 0.29 \text{ MeV}/c^2, \\
 m_{\Xi_b^0} - m_{\Lambda_b^0} &= 171.78 \pm 0.60 \pm 0.19 \pm 0.27 \text{ MeV}/c^2, \\
 m_{\Xi_b^-} - m_{\Lambda_b^0} &= 177.68 \pm 0.63 \pm 0.10 \pm 0.31 \text{ MeV}/c^2, \\
 m_{\Xi_b^-} - m_{\Xi_b^0} &= 5.90 \pm 0.87 \pm 0.22 \pm 0.23 \text{ MeV}/c^2,
 \end{aligned}$$

where the first uncertainties are statistical, the second systematic, and the third due to those on masses of Λ_c^+ , Ξ_c^+ , Ξ_c^0 , and D_s^- hadrons. The measurements are consistent with previous world averages [2], and comparisons are shown in Table 5 and Fig 2.

The relative production rates of the three $H_b \rightarrow H_c D_s$ decays, given in Eq. 1- 3, are

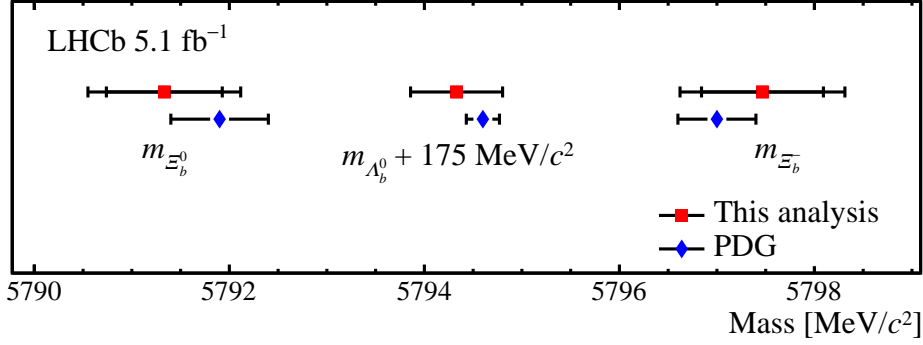


Figure 2: Comparison of measured (red) b baryon masses with (blue) the PDG values [2]. The mass of Λ_b^0 is shifted upward by $175 \text{ MeV}/c^2$ to reduce the range of this plot. The inner (outer) error bar is for the statistical (total) uncertainty.

Table 5: Measured H_b masses and mass differences and the previous world averages [2].

	This analysis [MeV/c^2]	Previous world average [MeV/c^2]
$m_{\Lambda_b^0}$	5619.34 ± 0.47	5619.60 ± 0.17
$m_{\Xi_b^0}$	5791.1 ± 0.8	5791.9 ± 0.5
$m_{\Xi_b^-}$	5797.0 ± 0.8	5797.0 ± 0.6
$m_{\Xi_b^0} - m_{\Lambda_b^0}$	171.8 ± 0.7	172.5 ± 0.4
$m_{\Xi_b^-} - m_{\Lambda_b^0}$	177.7 ± 0.7	177.46 ± 0.31
$m_{\Xi_b^-} - m_{\Xi_b^0}$	5.9 ± 0.9	5.9 ± 0.6

295 measured to be

$$\mathcal{R} \left(\frac{\Xi_b^0}{\Lambda_b^0} \right) = (15.8 \pm 1.1 \pm 0.6 \pm 7.7)\%,$$

$$\mathcal{R} \left(\frac{\Xi_b^-}{\Lambda_b^0} \right) = (16.9 \pm 1.3 \pm 0.9 \pm 4.3)\%,$$

$$\mathcal{R} \left(\frac{\Xi_b^0}{\Xi_b^-} \right) = (93.6 \pm 9.6 \pm 6.1 \pm 51.0)\%,$$

296 where the first uncertainties are statistical, the second systematic, and the third due to
 297 those on the branching fractions of Λ_c^+ , Ξ_c^+ , and Ξ_c^0 decays. Figure 3 shows the measured
 298 \mathcal{R} values. The results are consistent with the $SU(3)$ flavour symmetry and predictions of
 299 phenomenological models [33, 34].

300 7 Summary

301 In this analysis, the dicharm decays of Ξ_b baryons $\Xi_b^0 \rightarrow \Xi_c^+ D_s^-$ and $\Xi_b^- \rightarrow \Xi_c^0 D_s^-$ are
 302 observed for the first time, using proton-proton collision data collected by the LHCb
 303 experiment at a centre-of-mass energy of $\sqrt{s} = 13 \text{ TeV}$, corresponding to an integrated
 304 luminosity of 5.1 fb^{-1} . The masses of the Λ_b^0 , Ξ_b^0 and Ξ_b^- baryons are measured through
 305 these two decays, and are consistent with known values [2]. These measurements will

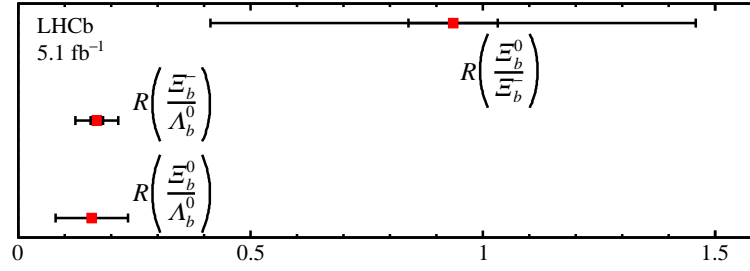


Figure 3: Measured \mathcal{R} values. The inner (outer) error bar is for the statistical (total) uncertainty.

306 improve the world averages. The relative branching fractions of these two decays are also
 307 measured. The results are consistent with $SU(3)$ flavour symmetry and several predictions
 308 for relative production rates and decay branching fractions of b baryons [6, 33–35].

Acknowledgements

We express our gratitude to our colleagues in the CERN accelerator departments for the excellent performance of the LHC. We thank the technical and administrative staff at the LHCb institutes. We acknowledge support from CERN and from the national agencies: CAPES, CNPq, FAPERJ and FINEP (Brazil); MOST and NSFC (China); CNRS/IN2P3 (France); BMBF, DFG and MPG (Germany); INFN (Italy); NWO (Netherlands); MNiSW and NCN (Poland); MEN/IFA (Romania); MICINN (Spain); SNSF and SER (Switzerland); NASU (Ukraine); STFC (United Kingdom); DOE NP and NSF (USA). We acknowledge the computing resources that are provided by CERN, IN2P3 (France), KIT and DESY (Germany), INFN (Italy), SURF (Netherlands), PIC (Spain), GridPP (United Kingdom), CSCS (Switzerland), IFIN-HH (Romania), CBPF (Brazil), Polish WLCG (Poland) and NERSC (USA). We are indebted to the communities behind the multiple open-source software packages on which we depend. Individual groups or members have received support from ARC and ARDC (Australia); Minciencias (Colombia); AvH Foundation (Germany); EPLANET, Marie Skłodowska-Curie Actions, ERC and NextGenerationEU (European Union); A*MIDEX, ANR, IPhU and Labex P2IO, and Région Auvergne-Rhône-Alpes (France); Key Research Program of Frontier Sciences of CAS, CAS PIFI, CAS CCEPP, Fundamental Research Funds for the Central Universities, and Sci. & Tech. Program of Guangzhou (China); GVA, XuntaGal, GENCAT, Inditex, InTalent and Prog. Atracción Talento, CM (Spain); SRC (Sweden); the Leverhulme Trust, the Royal Society and UKRI (United Kingdom).

Appendices

A Non-dicharm contribution

Three distinct sources of non-dicharm backgrounds are considered:

- The $H_b \rightarrow (pK^-(K^-)\pi^+)(K^+K^-\pi^+)$ decay with neither the H_c nor the D_s^- hadrons.
- The $H_b \rightarrow (pK^-(K^-)\pi^+)D_s^-$ decay without the H_c baryon.
- The $H_b \rightarrow H_c(K^+K^-\pi^+)$ decay without the D_s^- meson.

Figure 4 shows the two-dimensional H_c versus D_s^- invariant-mass distribution in the signal region and the H_c and/or D_s^- sideband regions. There are four regions illustrated in Fig 4:

- The region 1 lies in the H_c and D_s^- sideband region.
- The region 2 lies in the H_c signal and D_s^- sideband region.
- The region 3 lies in the H_c sideband and D_s^- signal region.
- The region 4 lies in the H_c and D_s^- signal region.

The H_b signal yields in the H_c and/or D_s^- sideband regions are estimated by simultaneous fitting to the H_b invariant-mass spectra in these four regions. The fit model is similar as the one mentioned in Sec. 4. Figures 5, 6, and 7 show the Λ_b^0 , Ξ_b^0 , and Ξ_b^- invariant-mass distributions in the H_c and/or D_s^- sideband regions superimposed by the fit results, respectively.

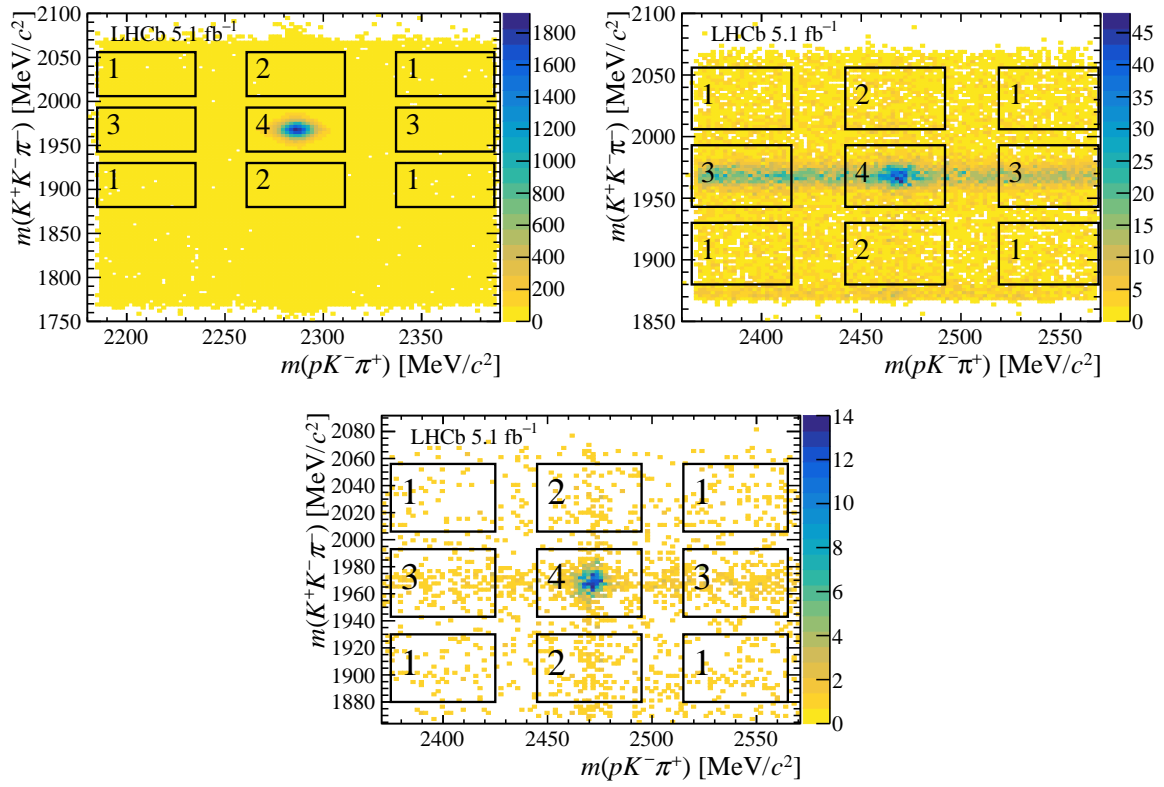


Figure 4: Distributions of the H_c mass versus the D_s^- mass with the regions 1–4 indicated. The regions illustrate the signal region and the H_c and/or D_s^- sideband regions.

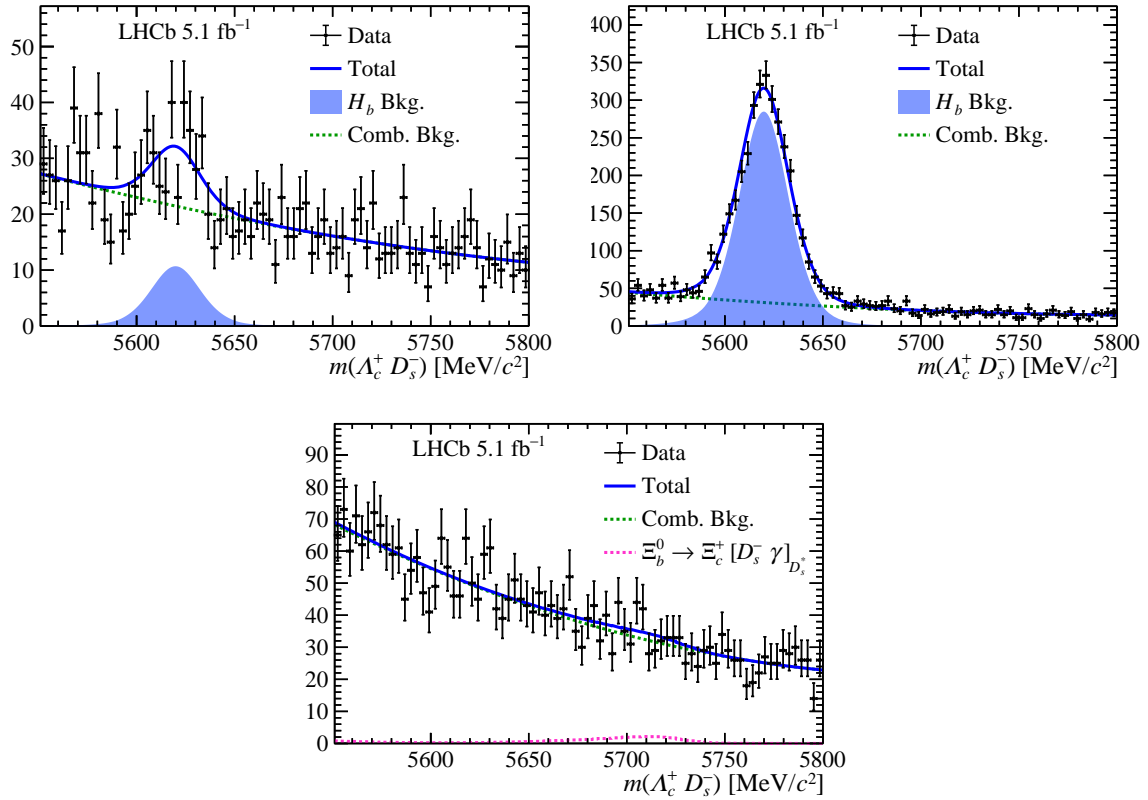


Figure 5: Invariant-mass distributions of Λ_b^0 candidates in the (top left) region 1, (top right) region 2, and (bottom) region 3.

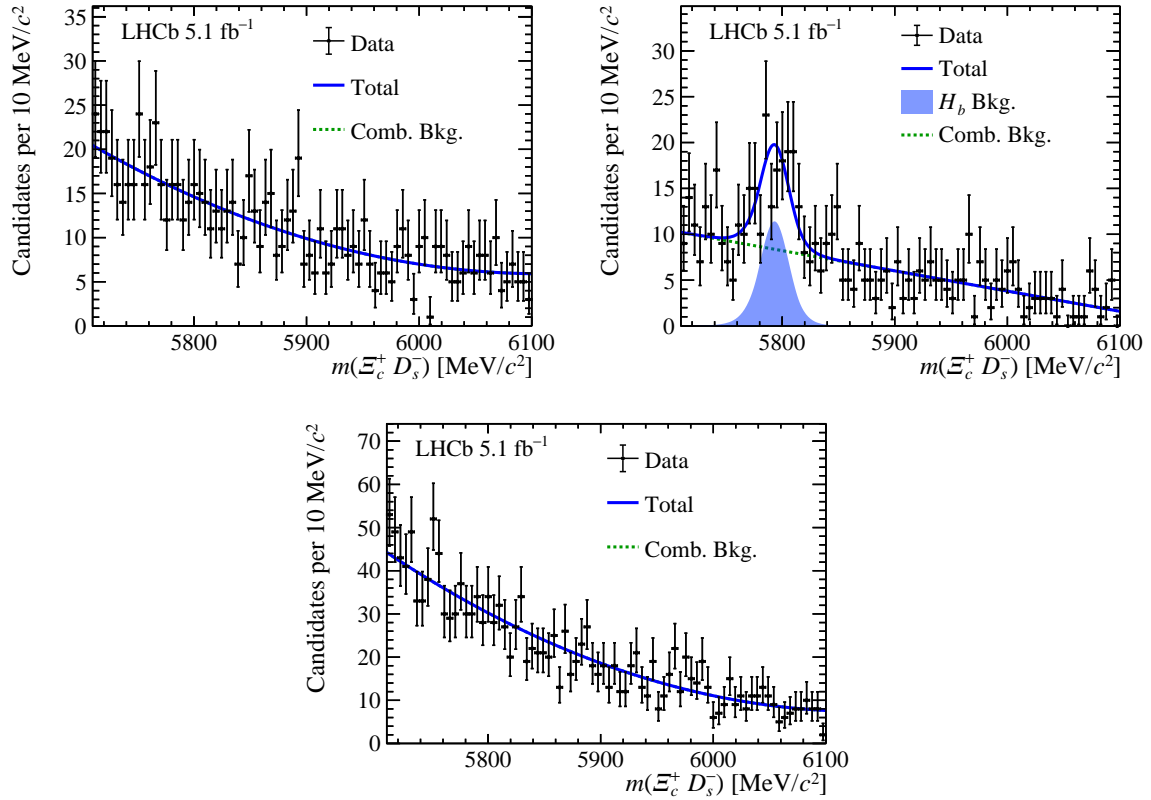


Figure 6: Invariant-mass distributions of Λ_b^0 candidates in the (top left) region 1, (top right) region 2, and (bottom) region 3.

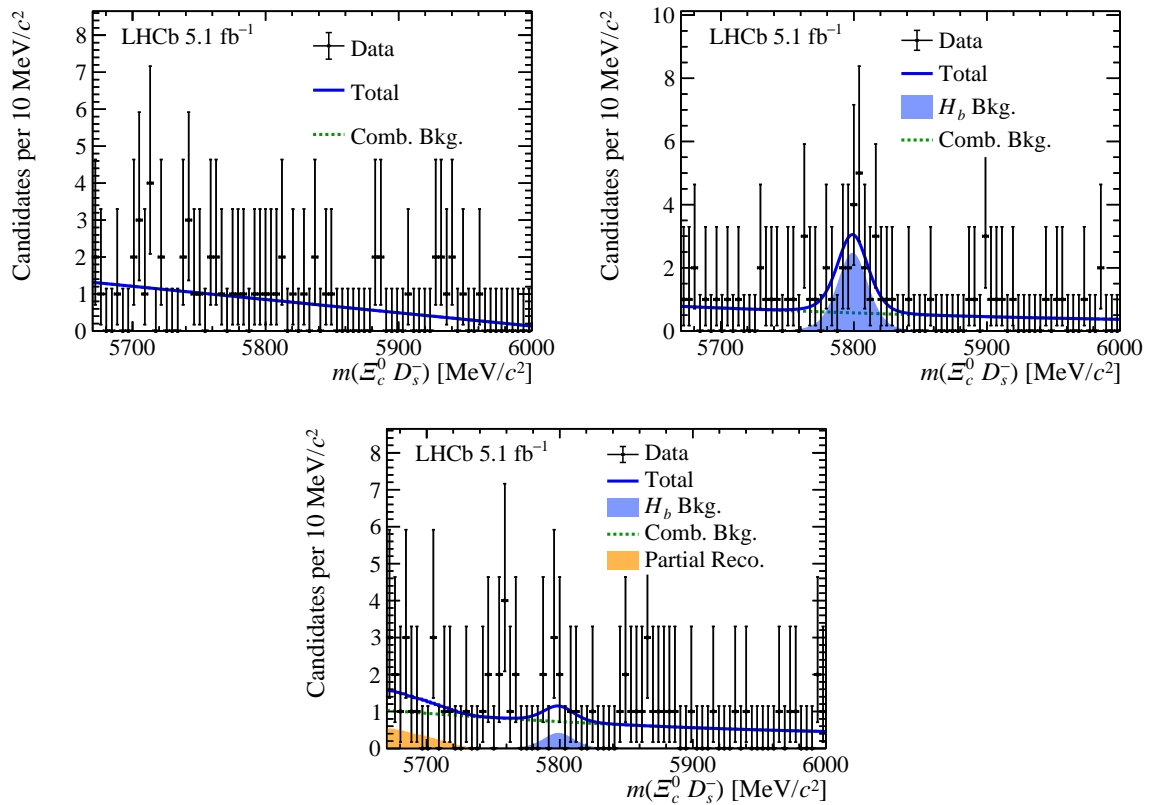


Figure 7: Invariant-mass distributions of Λ_b^0 candidates in the (top left) region 1, (top right) region 2, and (bottom) region 3.

References

- [1] S. Chen *et al.*, *Heavy flavour physics and CP violation at LHCb: a ten-year review*, Front. Phys. **18** (2023) 44601, [arXiv:2111.14360](#).
- [2] Particle Data Group, R. L. Workman *et al.*, *Review of particle physics*, Prog. Theor. Exp. Phys. **2022** (2022) 083C01.
- [3] A. Lenz, *Lifetimes and heavy quark expansion*, Int. J. Mod. Phys. A **30** (2015) 1543005, [arXiv:1405.3601](#).
- [4] M. Neubert, *B decays and the heavy quark expansion*, Adv. Ser. Direct. High Energy Phys. **15** (1998) 239, [arXiv:hep-ph/9702375](#).
- [5] M. Neubert, *Heavy quark symmetry*, Phys. Rept. **245** (1994) 259, [arXiv:hep-ph/9306320](#).
- [6] C.-K. Chua, *Color-allowed bottom baryon to s-wave and p-wave charmed baryon nonleptonic decays*, Phys. Rev. D **100** (2019) 034025, [arXiv:1905.00153](#).
- [7] LHCb collaboration, R. Aaij *et al.*, *Study of beauty hadron decays into pairs of charm hadrons*, Phys. Rev. Lett. **112** (2014) 202001, [arXiv:1403.3606](#).
- [8] LHCb collaboration, R. Aaij *et al.*, *Measurement of b hadron production fractions in 7 TeV pp collisions*, Phys. Rev. **D85** (2012) 032008, [arXiv:1111.2357](#).
- [9] LHCb collaboration, R. Aaij *et al.*, *Study of the kinematic dependences of Λ_b^0 production in pp collisions and a measurement of the $\Lambda_b^0 \rightarrow \Lambda_c^+ \pi^-$ branching fraction*, JHEP **08** (2014) 143, [arXiv:1405.6842](#).
- [10] LHCb collaboration, R. Aaij *et al.*, *Measurement of b-hadron fractions in 13 TeV pp collisions*, Phys. Rev. **D100** (2019) 031102(R), [arXiv:1902.06794](#).
- [11] LHCb collaboration, R. Aaij *et al.*, *Measurement of the mass and production rate of Ξ_b^- baryons*, Phys. Rev. **D99** (2019) 052006, [arXiv:1901.07075](#).
- [12] LHCb collaboration, R. Aaij *et al.*, *LHCb detector performance*, Int. J. Mod. Phys. **A30** (2015) 1530022, [arXiv:1412.6352](#).
- [13] LHCb collaboration, A. A. Alves Jr. *et al.*, *The LHCb detector at the LHC*, JINST **3** (2008) S08005.
- [14] LHCb collaboration, R. Aaij *et al.*, *Measurement of the Λ_b^0 , Ξ_b^- and Ω_b^- baryon masses*, Phys. Rev. Lett. **110** (2013) 182001, [arXiv:1302.1072](#).
- [15] LHCb collaboration, R. Aaij *et al.*, *Precision measurement of D meson mass differences*, JHEP **06** (2013) 065, [arXiv:1304.6865](#).
- [16] R. Aaij *et al.*, *Performance of the LHCb trigger and full real-time reconstruction in Run 2 of the LHC*, JINST **14** (2019) P04013, [arXiv:1812.10790](#).

- 381 [17] T. Sjöstrand, S. Mrenna, and P. Skands, *A brief introduction to PYTHIA 8.1*, Comput.
382 Phys. Commun. **178** (2008) 852, arXiv:0710.3820.
- 383 [18] D. J. Lange, *The EvtGen particle decay simulation package*, Nucl. Instrum. Meth.
384 **A462** (2001) 152.
- 385 [19] N. Davidson, T. Przedzinski, and Z. Was, *PHOTOS interface in C++: Technical
386 and physics documentation*, Comp. Phys. Comm. **199** (2016) 86, arXiv:1011.0937.
- 387 [20] Geant4 collaboration, J. Allison *et al.*, *Geant4 developments and applications*, IEEE
388 Trans. Nucl. Sci. **53** (2006) 270.
- 389 [21] LHCb collaboration, M. Clemencic *et al.*, *The LHCb simulation application, Gauss:
390 Design, evolution and experience*, J. Phys. Conf. Ser. **331** (2011) 032023.
- 391 [22] R. Aaij *et al.*, *Selection and processing of calibration samples to measure the particle
392 identification performance of the LHCb experiment in Run 2*, Eur. Phys. J. Tech.
393 Instr. **6** (2019) 1, arXiv:1803.00824.
- 394 [23] Y. Freund and R. E. Schapire, *A decision-theoretic generalization of on-line learning
395 and an application to boosting*, J. Comput. Syst. Sci. **55** (1997) 119.
- 396 [24] R. H. Dalitz, *On the analysis of τ -meson data and the nature of the τ -meson*, Phil.
397 Mag. Ser. 7 **44** (1953) 1068.
- 398 [25] LHCb collaboration, R. Aaij *et al.*, *Measurement of the track reconstruction efficiency
399 at LHCb*, JINST **10** (2015) P02007, arXiv:1408.1251.
- 400 [26] A. Rogozhnikov, *Reweighting with boosted decision trees*, J. Phys. Conf. Ser. **762**
401 (2016) 012036, arXiv:1608.05806, https://github.com/arogozhnikov/hep_ml.
- 402 [27] W. D. Hulsbergen, *Decay chain fitting with a Kalman filter*, Nucl. Instrum. Meth.
403 **A552** (2005) 566, arXiv:physics/0503191.
- 404 [28] T. Skwarnicki, *A study of the radiative cascade transitions between the Upsilon-prime
405 and Upsilon resonances*, PhD thesis, Institute of Nuclear Physics, Krakow, 1986,
406 DESY-F31-86-02.
- 407 [29] C. Abellan Beteta *et al.*, *Calibration and performance of the LHCb calorimeters in
408 Run 1 and 2 at the LHC*, arXiv:2008.11556, submitted to JINST.
- 409 [30] LHCb collaboration, R. Aaij *et al.*, *Measurement of the track reconstruction efficiency
410 at LHCb*, JINST **10** (2015) P02007, arXiv:1408.1251.
- 411 [31] LHCb collaboration, R. Aaij *et al.*, *Measurement of b-hadron masses*, Phys. Lett.
412 **B708** (2012) 241, arXiv:1112.4896.
- 413 [32] LHCb collaboration, R. Aaij *et al.*, *Precision measurement of D meson mass differ-
414 ences*, JHEP **06** (2013) 065, arXiv:1304.6865.
- 415 [33] Y. K. Hsiao, P. Y. Lin, L. W. Luo, and C. Q. Geng, *Fragmentation fractions of
416 two-body b-baryon decays*, Phys. Lett. B **751** (2015) 127, arXiv:1510.01808.

- 417 [34] H.-Y. Jiang and F.-S. Yu, *Fragmentation-fraction ratio f_{Ξ_b}/f_{Λ_b} in b - and c -baryon*
418 *decays*, Eur. Phys. J. C **78** (2018) 224, arXiv:1802.02948.
- 419 [35] Y.-S. Li and X. Liu, *Restudy of the color-allowed two-body nonleptonic decays of*
420 *bottom baryons Ξ_b and Ω_b supported by hadron spectroscopy*, Phys. Rev. D **105** (2022)
421 013003, arXiv:2112.02481.




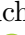



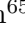




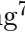
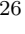


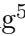





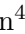



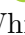





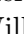



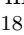
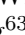
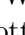
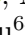


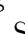
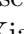


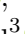





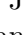


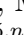
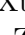

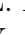
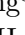







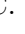

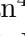
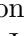
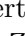
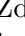



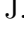
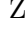
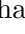


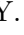
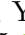

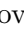






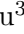


LHCb collaboration

422 R. Aaij³³ , A.S.W. Abdelmotteleb⁵² , C. Abellan Beteta⁴⁶ , F. Abudinén⁵² ,
 423 T. Ackernley⁵⁶ , B. Adeva⁴² , M. Adinolfi⁵⁰ , P. Adlarson⁷⁸ , H. Afsharnia¹⁰ ,
 424 C. Agapopoulou⁴⁴ , C.A. Aidala⁷⁹ , Z. Ajaltouni¹⁰ , S. Akar⁶¹ , K. Akiba³³ ,
 425 P. Albicocco²⁴ , J. Albrecht¹⁶ , F. Alessio⁴⁴ , M. Alexander⁵⁵ , A. Alfonso Alberro⁴¹ ,
 426 Z. Aliouche⁵⁸ , P. Alvarez Cartelle⁵¹ , R. Amalric¹⁴ , S. Amato² , J.L. Amey⁵⁰ ,
 427 Y. Amhis^{12,44} , L. An⁵ , L. Anderlini²³ , M. Andersson⁴⁶ , A. Andreianov³⁹ ,
 428 P. Andreola⁴⁶ , M. Andreotti²² , D. Andreou⁶⁴ , D. Ao⁶ , F. Archilli^{32,v} ,
 429 S. Arguedas Cuendis⁸ , A. Artamonov³⁹ , M. Artuso⁶⁴ , E. Aslanides¹¹ , M. Atzeni⁶⁰ ,
 430 B. Audurier¹³ , D. Bacher⁵⁹ , I. Bachiller Perea⁹ , S. Bachmann¹⁸ , M. Bachmayer⁴⁵ ,
 431 J.J. Back⁵² , A. Bailly-reyre¹⁴ , P. Baladron Rodriguez⁴² , V. Balagura¹³ ,
 432 W. Baldini^{22,44} , J. Baptista de Souza Leite¹ , M. Barbetti^{23,m} , I. R. Barbosa⁶⁶ ,
 433 R.J. Barlow⁵⁸ , S. Barsuk¹² , W. Barter⁵⁴ , M. Bartolini⁵¹ , F. Baryshnikov³⁹ ,
 434 J.M. Basels¹⁵ , G. Bassi^{30,s} , B. Batsukh⁴ , A. Battig¹⁶ , A. Bay⁴⁵ , A. Beck⁵² ,
 435 M. Becker¹⁶ , F. Bedeschi³⁰ , I.B. Bediaga¹ , A. Beiter⁶⁴ , S. Belin⁴² , V. Bellee⁴⁶ ,
 436 K. Belous³⁹ , I. Belov²⁵ , I. Belyaev³⁹ , G. Benane¹¹ , G. Bencivenni²⁴ ,
 437 E. Ben-Haim¹⁴ , A. Berezhnoy³⁹ , R. Bernet⁴⁶ , S. Bernet Andres⁴⁰ , D. Berninghoff¹⁸ ,
 438 H.C. Bernstein⁶⁴ , C. Bertella⁵⁸ , A. Bertolin²⁹ , C. Betancourt⁴⁶ , F. Betti⁵⁴ , J.
 439 Bex⁵¹ , Ia. Bezshyiko⁴⁶ , J. Bhom³⁶ , L. Bian⁷⁰ , M.S. Bieker¹⁶ , N.V. Biesuz²² ,
 440 P. Billoir¹⁴ , A. Biolchini³³ , M. Birch⁵⁷ , F.C.R. Bishop⁵¹ , A. Bitadze⁵⁸ ,
 441 A. Bizzeti , M.P. Blago⁵¹ , T. Blake⁵² , F. Blanc⁴⁵ , J.E. Blank¹⁶ , S. Blusk⁶⁴ ,
 442 D. Bobulska⁵⁵ , V. Bocharnikov³⁹ , J.A. Boelhauve¹⁶ , O. Boente Garcia¹³ ,
 443 T. Boettcher⁶¹ , A. Bohare⁵⁴ , A. Boldyrev³⁹ , C.S. Bolognani⁷⁶ , R. Bolzonella^{22,l} ,
 444 N. Bondar³⁹ , F. Borgato^{29,44} , S. Borghi⁵⁸ , M. Borsato¹⁸ , J.T. Borsuk³⁶ ,
 445 S.A. Bouchiba⁴⁵ , T.J.V. Bowcock⁵⁶ , A. Boyer⁴⁴ , C. Bozzi²² , M.J. Bradley⁵⁷ ,
 446 S. Braun⁶² , A. Brea Rodriguez⁴² , N. Breer¹⁶ , J. Brodzicka³⁶ , A. Brossa Gonzalo⁴² ,
 447 J. Brown⁵⁶ , D. Brundu²⁸ , A. Buonauro⁴⁶ , L. Buonincontri²⁹ , A.T. Burke⁵⁸ ,
 448 C. Burr⁴⁴ , A. Bursche⁶⁸ , A. Butkevich³⁹ , J.S. Butter³³ , J. Buytaert⁴⁴ ,
 449 W. Byczynski⁴⁴ , S. Cadeddu²⁸ , H. Cai⁷⁰ , R. Calabrese^{22,l} , L. Calefice¹⁶ , S. Cali²⁴ ,
 450 M. Calvi^{27,p} , M. Calvo Gomez⁴⁰ , J. Cambon Bouzas⁴² , P. Campana²⁴ ,
 451 D.H. Campora Perez⁷⁶ , A.F. Campoverde Quezada⁶ , S. Capelli^{27,p} , L. Capriotti²² ,
 452 A. Carbone^{21,j} , L. Carcedo Salgado⁴² , R. Cardinale^{25,n} , A. Cardini²⁸ , P. Carniti^{27,p} ,
 453 L. Carus¹⁸ , A. Casais Vidal⁴² , R. Caspary¹⁸ , G. Casse⁵⁶ , M. Cattaneo⁴⁴ ,
 454 G. Cavallero²² , V. Cavallini^{22,l} , S. Celani⁴⁵ , J. Cerasoli¹¹ , D. Cervenkov⁵⁹ , S.
 455 Cesare^{26,o} , A.J. Chadwick⁵⁶ , I. Chahrouh⁷⁹ , M.G. Chapman⁵⁰ , M. Charles¹⁴ ,
 456 Ph. Charpentier⁴⁴ , C.A. Chavez Barajas⁵⁶ , M. Chefdeville⁹ , C. Chen¹¹ , S. Chen⁴ ,
 457 A. Chernov³⁶ , S. Chernyshenko⁴⁸ , V. Chobanova^{42,z} , S. Cholak⁴⁵ , M. Chrzaszcz³⁶ ,
 458 A. Chubykin³⁹ , V. Chulikov³⁹ , P. Ciambone²⁴ , M.F. Cicala⁵² , X. Cid Vidal⁴² ,
 459 G. Ciezarek⁴⁴ , P. Cifra⁴⁴ , P.E.L. Clarke⁵⁴ , M. Clemencic⁴⁴ , H.V. Cliff⁵¹ ,
 460 J. Closier⁴⁴ , J.L. Cobbledick⁵⁸ , C. Cocha Toapaxi¹⁸ , V. Coco⁴⁴ , J. Cogan¹¹ ,
 461 E. Cogneras¹⁰ , L. Cojocariu³⁸ , P. Collins⁴⁴ , T. Colombo⁴⁴ , A. Comerma-Montells⁴¹ ,
 462 L. Congedo²⁰ , A. Contu²⁸ , N. Cooke⁵⁵ , I. Corredoira⁴² , A. Correia¹⁴ , G. Corti⁴⁴ ,
 463 J.J. Cottee Meldrum⁵⁰ , B. Couturier⁴⁴ , D.C. Craik⁴⁶ , M. Cruz Torres^{1,h} , R. Currie⁵⁴ ,
 464 C.L. Da Silva⁶³ , S. Dadabaev³⁹ , L. Dai⁶⁷ , X. Dai⁵ , E. Dall'Occo¹⁶ , J. Dalseno⁴² ,
 465 C. D'Ambrosio⁴⁴ , J. Daniel¹⁰ , A. Danilina³⁹ , P. d'Argent²⁰ , A. Davidson⁵² ,
 466 J.E. Davies⁵⁸ , A. Davis⁵⁸ , O. De Aguiar Francisco⁵⁸ , C. De Angelis^{28,k} , J. de Boer³³ ,
 467 K. De Bruyn⁷⁵ , S. De Capua⁵⁸ , M. De Cian¹⁸ , U. De Freitas Carneiro Da Graca^{1,b} ,
 468 E. De Lucia²⁴ , J.M. De Miranda¹ , L. De Paula² , M. De Serio^{20,i} , D. De Simone⁴⁶ ,
 469 P. De Simone²⁴ , F. De Vellis¹⁶ , J.A. de Vries⁷⁶ , C.T. Dean⁶³ , F. Debernardis^{20,i} ,

470 D. Decamp⁹ , V. Dedu¹¹ , L. Del Buono¹⁴ , B. Delaney⁶⁰ , H.-P. Dembinski¹⁶ ,
 471 J. Deng⁷ , V. Denysenko⁴⁶ , O. Deschamps¹⁰ , F. Dettori^{28,k} , B. Dey⁷³ ,
 472 P. Di Nezza²⁴ , I. Diachkov³⁹ , S. Didenko³⁹ , S. Ding⁶⁴ , V. Dobishuk⁴⁸ , A. D.
 473 Docheva⁵⁵ , A. Dolmatov³⁹ , C. Dong³ , A.M. Donohoe¹⁹ , F. Dordei²⁸ ,
 474 A.C. dos Reis¹ , L. Douglas⁵⁵ , A.G. Downes⁹ , W. Duan⁶⁸ , P. Duda⁷⁷ ,
 475 M.W. Dudek³⁶ , L. Dufour⁴⁴ , V. Duk⁷⁴ , P. Durante⁴⁴ , M. M. Duras⁷⁷ ,
 476 J.M. Durham⁶³ , D. Dutta⁵⁸ , A. Dziurda³⁶ , A. Dzyuba³⁹ , S. Easo^{53,44} ,
 477 E. Eckstein⁷² , U. Egede⁶⁵ , A. Egorychev³⁹ , V. Egorychev³⁹ , C. Eirea Orro⁴²,
 478 S. Eisenhardt⁵⁴ , E. Ejopu⁵⁸ , S. Ek-In⁴⁵ , L. Eklund⁷⁸ , M. Elashri⁶¹ ,
 479 J. Ellbracht¹⁶ , S. Ely⁵⁷ , A. Ene³⁸ , E. Epple⁶¹ , S. Escher¹⁵ , J. Eschle⁴⁶ ,
 480 S. Esen⁴⁶ , T. Evans⁵⁸ , F. Fabiano^{28,k,44} , L.N. Falcao¹ , Y. Fan⁶ , B. Fang^{70,12} ,
 481 L. Fantini^{74,r} , M. Faria⁴⁵ , K. Farmer⁵⁴ , S. Farry⁵⁶ , D. Fazzini^{27,p} ,
 482 L. Felkowski⁷⁷ , M. Feng^{4,6} , M. Feo⁴⁴ , M. Fernandez Gomez⁴² , A.D. Fernez⁶² ,
 483 F. Ferrari²¹ , L. Ferreira Lopes⁴⁵ , F. Ferreira Rodrigues² , S. Ferreres Sole³³ ,
 484 M. Ferrillo⁴⁶ , M. Ferro-Luzzi⁴⁴ , S. Filippov³⁹ , R.A. Fini²⁰ , M. Fiorini^{22,l} ,
 485 M. Firlej³⁵ , K.M. Fischer⁵⁹ , D.S. Fitzgerald⁷⁹ , C. Fitzpatrick⁵⁸ , T. Fiutowski³⁵ ,
 486 F. Fleuret¹³ , M. Fontana²¹ , F. Fontanelli^{25,n} , L. F. Foreman⁵⁸ , R. Forty⁴⁴ ,
 487 D. Foulds-Holt⁵¹ , M. Franco Sevilla⁶² , M. Frank⁴⁴ , E. Franzoso^{22,l} , G. Frau¹⁸ ,
 488 C. Frei⁴⁴ , D.A. Friday⁵⁸ , L. Frontini^{26,o} , J. Fu⁶ , Q. Fuehring¹⁶ , Y. Fujii⁶⁵ ,
 489 T. Fulghesu¹⁴ , E. Gabriel³³ , G. Galati^{20,i} , M.D. Galati³³ , A. Gallas Torreira⁴² ,
 490 D. Galli^{21,j} , S. Gambetta^{54,44} , M. Gandelman² , P. Gandini²⁶ , H. Gao⁶ ,
 491 R. Gao⁵⁹ , Y. Gao⁷ , Y. Gao⁵ , Y. Gao⁷ , M. Garau^{28,k} , L.M. Garcia Martin⁴⁵ ,
 492 P. Garcia Moreno⁴¹ , J. García Pardiñas⁴⁴ , B. Garcia Plana⁴², F.A. Garcia Rosales¹³ ,
 493 L. Garrido⁴¹ , C. Gaspar⁴⁴ , R.E. Geertsema³³ , L.L. Gerken¹⁶ , E. Gersabeck⁵⁸ ,
 494 M. Gersabeck⁵⁸ , T. Gershon⁵² , Z. Ghorbanimoghaddam⁵⁰, L. Giambastiani²⁹ , F. I.
 495 Giasemis^{14,f} , V. Gibson⁵¹ , H.K. Gienza³⁷ , A.L. Gilman⁵⁹ , M. Giovannetti²⁴ ,
 496 A. Gioventù⁴² , P. Gironella Gironell⁴¹ , C. Giugliano^{22,l} , M.A. Giza³⁶ , K. Gizdov⁵⁴ ,
 497 E.L. Gkougkousis⁴⁴ , F.C. Glaser^{12,18} , V.V. Gligorov¹⁴ , C. Göbel⁶⁶ , E. Golobardes⁴⁰ ,
 498 D. Golubkov³⁹ , A. Golutvin^{57,39,44} , A. Gomes^{1,2,c,a,†} , S. Gomez Fernandez⁴¹ ,
 499 F. Goncalves Abrantes⁵⁹ , M. Goncerz³⁶ , G. Gong³ , J. A. Gooding¹⁶ , I.V. Gorelov³⁹ ,
 500 C. Gotti²⁷ , J.P. Grabowski⁷² , L.A. Granado Cardoso⁴⁴ , E. Graugés⁴¹ ,
 501 E. Graverini⁴⁵ , L. Grazette⁵² , G. Graziani , A. T. Grecu³⁸ , L.M. Greeven³³ ,
 502 N.A. Grieser⁶¹ , L. Grillo⁵⁵ , S. Gromov³⁹ , C. Gu¹³ , M. Guarise²² , M. Guittiere¹² ,
 503 V. Guliaeva³⁹ , P. A. Günther¹⁸ , A.-K. Guseinov³⁹ , E. Gushchin³⁹ , Y. Guz^{5,39,44} ,
 504 T. Gys⁴⁴ , T. Hadavizadeh⁶⁵ , C. Hadjivasiliou⁶² , G. Haefeli⁴⁵ , C. Haen⁴⁴ ,
 505 J. Haimberger⁴⁴ , S.C. Haines⁵¹ , M. Hajheidari⁴⁴, T. Halewood-leagas⁵⁶ ,
 506 M.M. Halvorsen⁴⁴ , P.M. Hamilton⁶² , J. Hammerich⁵⁶ , Q. Han⁷ , X. Han¹⁸ ,
 507 S. Hansmann-Menzemer¹⁸ , L. Hao⁶ , N. Harnew⁵⁹ , T. Harrison⁵⁶ , M. Hartmann¹² ,
 508 C. Hasse⁴⁴ , M. Hatch⁴⁴ , J. He^{6,e} , K. Heijhoff³³ , F. Hemmer⁴⁴ , C. Henderson⁶¹ ,
 509 R.D.L. Henderson^{65,52} , A.M. Hennequin⁴⁴ , K. Hennessy⁵⁶ , L. Henry⁴⁵ , J. Herd⁵⁷ ,
 510 J. Heuel¹⁵ , A. Hicheur² , D. Hill⁴⁵ , M. Hilton⁵⁸ , S.E. Hollitt¹⁶ , J. Horswill⁵⁸ ,
 511 R. Hou⁷ , Y. Hou⁹ , N. Howarth⁵⁶, J. Hu¹⁸, J. Hu⁶⁸ , W. Hu⁵ , X. Hu³ , W. Huang⁶ ,
 512 X. Huang⁷⁰ , W. Hulsbergen³³ , R.J. Hunter⁵² , M. Hushchyn³⁹ , D. Hutchcroft⁵⁶ ,
 513 P. Ibis¹⁶ , M. Idzik³⁵ , D. Ilin³⁹ , P. Ilten⁶¹ , A. Inglessi³⁹ , A. Iniukhin³⁹ ,
 514 A. Ishteev³⁹ , K. Ivshin³⁹ , R. Jacobsson⁴⁴ , H. Jage¹⁵ , S.J. Jaimes Elles^{43,71} ,
 515 S. Jakobsen⁴⁴ , E. Jans³³ , B.K. Jashal⁴³ , A. Jawahery⁶² , V. Jevtic¹⁶ , E. Jiang⁶² ,
 516 X. Jiang^{4,6} , Y. Jiang⁶ , Y. J. Jiang⁵ , M. John⁵⁹ , D. Johnson⁴⁹ , C.R. Jones⁵¹ ,
 517 T.P. Jones⁵² , S. Joshi³⁷ , B. Jost⁴⁴ , N. Jurik⁴⁴ , I. Juszcak³⁶ , D. Kaminaris⁴⁵ ,
 518 S. Kandybei⁴⁷ , Y. Kang³ , M. Karacson⁴⁴ , D. Karpenkov³⁹ , M. Karpov³⁹ , A. M.
 519 Kauniskangas⁴⁵ , J.W. Kautz⁶¹ , F. Keizer⁴⁴ , D.M. Keller⁶⁴ , M. Kenzie⁵¹ ,

520 T. Ketel³³ , B. Khanji⁶⁴ , A. Kharisova³⁹ , S. Kholodenko³⁰ , G. Khreich¹² ,
521 T. Kirn¹⁵ , V.S. Kirsebom⁴⁵ , O. Kitouni⁶⁰ , S. Klaver³⁴ , N. Kleijne^{30,s} ,
522 K. Klimaszewski³⁷ , M.R. Kmiec³⁷ , S. Koliiev⁴⁸ , L. Kolk¹⁶ , A. Konoplyannikov³⁹ ,
523 P. Kopciwicz^{35,44} , R. Kopecna¹⁸ , P. Koppenburg³³ , M. Korolev³⁹ , I. Kostiuik³³ ,
524 O. Kot⁴⁸ , S. Kotriakhova , A. Kozachuk³⁹ , P. Kravchenko³⁹ , L. Kravchuk³⁹ ,
525 M. Kreps⁵² , S. Kretschmar¹⁵ , P. Krovovny³⁹ , W. Krupa⁶⁴ , W. Krzemien³⁷ ,
526 J. Kubat¹⁸ , S. Kubis⁷⁷ , W. Kucewicz³⁶ , M. Kucharczyk³⁶ , V. Kudryavtsev³⁹ ,
527 E. Kulikova³⁹ , A. Kupsc⁷⁸ , B. K. Kutsenko¹¹ , D. Lacarrere⁴⁴ , G. Lafferty⁵⁸ ,
528 A. Lai²⁸ , A. Lampis^{28,k} , D. Lancierini⁴⁶ , C. Landesa Gomez⁴² , J.J. Lane⁶⁵ ,
529 R. Lane⁵⁰ , C. Langenbruch¹⁸ , J. Langer¹⁶ , O. Lantwin³⁹ , T. Latham⁵² ,
530 F. Lazzari^{30,t} , C. Lazzeroni⁴⁹ , R. Le Gac¹¹ , S.H. Lee⁷⁹ , R. Lefèvre¹⁰ , A. Leflat³⁹ ,
531 S. Legotin³⁹ , O. Leroy¹¹ , T. Lesiak³⁶ , B. Leverington¹⁸ , A. Li³ , H. Li⁶⁸ ,
532 K. Li⁷ , L. Li⁵⁸ , P. Li⁴⁴ , P.-R. Li⁶⁹ , S. Li⁷ , T. Li⁴ , T. Li⁶⁸ , Y. Li⁷ , Y. Li⁴ ,
533 Z. Li⁶⁴ , Z. Lian³ , X. Liang⁶⁴ , C. Lin⁶ , T. Lin⁵³ , R. Lindner⁴⁴ , V. Lisovskiy⁴⁵ ,
534 R. Litvinov^{28,k} , G. Liu⁶⁸ , H. Liu⁶ , K. Liu⁶⁹ , Q. Liu⁶ , S. Liu^{4,6} , Y. Liu⁵⁴ ,
535 Y. Liu⁶⁹ , A. Lobo Salvia⁴¹ , A. Loi²⁸ , J. Lomba Castro⁴² , T. Long⁵¹ , I. Longstaff⁵⁵ ,
536 J.H. Lopes² , A. Lopez Huertas⁴¹ , S. López Soliño⁴² , G.H. Lovell⁵¹ , Y. Lu^{4,d} ,
537 C. Lucarelli^{23,m} , D. Lucchesi^{29,q} , S. Luchuk³⁹ , M. Lucio Martinez⁷⁶ ,
538 V. Lukashenko^{33,48} , Y. Luo³ , A. Lupato²⁹ , E. Luppi^{22,l} , K. Lynch¹⁹ , X.-R. Lyu⁶ ,
539 G. M. Ma³ , R. Ma⁶ , S. Maccolini¹⁶ , F. Machefert¹² , F. Maciuc³⁸ , I. Mackay⁵⁹ ,
540 L.R. Madhan Mohan⁵¹ , M. M. Madurai⁴⁹ , A. Maevskiy³⁹ , D. Magdalinski³³ ,
541 D. Maisuzenko³⁹ , M.W. Majewski³⁵ , J.J. Malczewski³⁶ , S. Malde⁵⁹ , B. Malecki^{36,44} ,
542 L. Malentacca⁴⁴ , A. Malinin³⁹ , T. Maltsev³⁹ , G. Manca^{28,k} , G. Mancinelli¹¹ ,
543 C. Mancuso^{26,12,o} , R. Manera Escalero⁴¹ , D. Manuzzi²¹ , D. Marangotto^{26,o} ,
544 J.F. Marchand⁹ , U. Marconi²¹ , S. Mariani⁴⁴ , C. Marin Benito^{41,44} , J. Marks¹⁸ ,
545 A.M. Marshall⁵⁰ , P.J. Marshall⁵⁶ , G. Martelli^{74,r} , G. Martellotti³¹ , L. Martinazzoli⁴⁴ ,
546 M. Martinelli^{27,p} , D. Martinez Santos⁴² , F. Martinez Vidal⁴³ , A. Massafferri¹ ,
547 M. Materok¹⁵ , R. Matev⁴⁴ , A. Mathad⁴⁶ , V. Matiunin³⁹ , C. Matteuzzi^{64,27} ,
548 K.R. Mattioli¹³ , A. Mauri⁵⁷ , E. Maurice¹³ , J. Mauricio⁴¹ , M. Mazurek⁴⁴ ,
549 M. McCann⁵⁷ , L. McConnell¹⁹ , T.H. McGrath⁵⁸ , N.T. McHugh⁵⁵ , A. McNab⁵⁸ ,
550 R. McNulty¹⁹ , B. Meadows⁶¹ , G. Meier¹⁶ , D. Melnychuk³⁷ , M. Merk^{33,76} ,
551 A. Merli^{26,o} , L. Meyer Garcia² , D. Miao^{4,6} , H. Miao⁶ , M. Mikhasenko^{72,g} ,
552 D.A. Milanese⁷¹ , A. Minotti^{27,p} , E. Minucci⁶⁴ , T. Miralles¹⁰ , S.E. Mitchell⁵⁴ ,
553 B. Mitreska¹⁶ , D.S. Mitzel¹⁶ , A. Modak⁵³ , A. Mödden¹⁶ , R.A. Mohammed⁵⁹ ,
554 R.D. Moise¹⁵ , S. Mokhnenko³⁹ , T. Mombächer⁴⁴ , M. Monk^{52,65} , I.A. Monroy⁷¹ ,
555 S. Monteil¹⁰ , A. Morcillo Gomez⁴² , G. Morello²⁴ , M.J. Morello^{30,s} ,
556 M.P. Morgenthaler¹⁸ , J. Moron³⁵ , A.B. Morris⁴⁴ , A.G. Morris¹¹ , R. Mountain⁶⁴ ,
557 H. Mu³ , Z. M. Mu⁵ , E. Muhammad⁵² , F. Muheim⁵⁴ , M. Mulder⁷⁵ , K. Müller⁴⁶ ,
558 F. Muñoz-Rojas⁸ , R. Murta⁵⁷ , P. Naik⁵⁶ , T. Nakada⁴⁵ , R. Nandakumar⁵³ ,
559 T. Nanut⁴⁴ , I. Nasteva² , M. Needham⁵⁴ , N. Neri^{26,o} , S. Neubert⁷² , N. Neufeld⁴⁴ ,
560 P. Neustroev³⁹ , R. Newcombe⁵⁷ , J. Nicolini^{16,12} , D. Nicotra⁷⁶ , E.M. Niel⁴⁵ ,
561 N. Nikitin³⁹ , P. Nogga⁷² , N.S. Nolte⁶⁰ , C. Normand^{9,k,28} , J. Novoa Fernandez⁴² ,
562 G. Nowak⁶¹ , C. Nunez⁷⁹ , H. N. Nur⁵⁵ , A. Oblakowska-Mucha³⁵ , V. Obraztsov³⁹ ,
563 T. Oeser¹⁵ , S. Okamura^{22,l,44} , R. Oldeman^{28,k} , F. Oliva⁵⁴ , M. Olocco¹⁶ ,
564 C.J.G. Onderwater⁷⁶ , R.H. O'Neil⁵⁴ , J.M. Otalora Goicochea² , T. Ovsiannikova³⁹ ,
565 P. Owen⁴⁶ , A. Oyanguren⁴³ , O. Ozcelik⁵⁴ , K.O. Padeken⁷² , B. Pagare⁵² ,
566 P.R. Pais¹⁸ , T. Pajero⁵⁹ , A. Palano²⁰ , M. Palutan²⁴ , G. Panshin³⁹ , L. Paolucci⁵² ,
567 A. Papanestis⁵³ , M. Pappagallo^{20,i} , L.L. Pappalardo^{22,l} , C. Pappenheimer⁶¹ ,
568 C. Parkes^{58,44} , B. Passalacqua^{22,l} , G. Passaleva²³ , D. Passaro^{30,s} , A. Pastore²⁰ ,
569 M. Patel⁵⁷ , J. Patoc⁵⁹ , C. Patrignani^{21,j} , C.J. Pawley⁷⁶ , A. Pellegrino³³ ,

570 M. Pepe Altarelli²⁴ , S. Perazzini²¹ , D. Pereima³⁹ , A. Pereiro Castro⁴² , P. Perret¹⁰ ,
571 A. Perro⁴⁴ , K. Petridis⁵⁰ , A. Petrolini^{25,n} , S. Petrucci⁵⁴ , H. Pham⁶⁴ , L. Pica^{30,s} ,
572 M. Piccini⁷⁴ , B. Pietrzyk⁹ , G. Pietrzyk¹² , D. Pinci³¹ , F. Pisani⁴⁴ ,
573 M. Pizzichemi^{27,p} , V. Placinta³⁸ , M. Plo Casasus⁴² , F. Polci^{14,44} , M. Poli Lener²⁴ ,
574 A. Poluektov¹¹ , N. Polukhina³⁹ , I. Polyakov⁴⁴ , E. Polycarpo² , S. Ponce⁴⁴ ,
575 D. Popov⁶ , S. Poslavskii³⁹ , K. Prasanth³⁶ , L. Promberger¹⁸ , C. Prouve⁴² ,
576 V. Pugatch⁴⁸ , V. Puill¹² , G. Punzi^{30,t} , H.R. Qi³ , W. Qian⁶ , N. Qin³ , S. Qu³ ,
577 R. Quagliani⁴⁵ , B. Rachwal³⁵ , J.H. Rademacker⁵⁰ , M. Rama³⁰ , M.
578 Ramírez García⁷⁹ , M. Ramos Pernas⁵² , M.S. Rangel² , F. Ratnikov³⁹ , G. Raven³⁴ ,
579 M. Rebollo De Miguel⁴³ , F. Redi⁴⁴ , J. Reich⁵⁰ , F. Reiss⁵⁸ , Z. Ren³ ,
580 P.K. Resmi⁵⁹ , R. Ribatti^{30,s} , G. R. Ricart^{13,80} , D. Riccardi^{30,s} , S. Ricciardi⁵³ ,
581 K. Richardson⁶⁰ , M. Richardson-Slipper⁵⁴ , K. Rinnert⁵⁶ , P. Robbe¹² ,
582 G. Robertson⁵⁴ , E. Rodrigues^{56,44} , E. Rodriguez Fernandez⁴² ,
583 J.A. Rodriguez Lopez⁷¹ , E. Rodriguez Rodriguez⁴² , A. Rogovskiy⁵³ , D.L. Rolf⁴⁴ ,
584 A. Rollings⁵⁹ , P. Roloff⁴⁴ , V. Romanovskiy³⁹ , M. Romero Lamas⁴² ,
585 A. Romero Vidal⁴² , G. Romolini²² , F. Ronchetti⁴⁵ , M. Rotondo²⁴ , M.S. Rudolph⁶⁴ ,
586 T. Ruf⁴⁴ , R.A. Ruiz Fernandez⁴² , J. Ruiz Vidal⁴³ , A. Ryzhikov³⁹ , J. Ryzka³⁵ ,
587 J.J. Saborido Silva⁴² , N. Sagidova³⁹ , N. Sahoo⁴⁹ , B. Saitta^{28,k} , M. Salomoni⁴⁴ ,
588 C. Sanchez Gras³³ , I. Sanderswood⁴³ , R. Santacesaria³¹ , C. Santamarina Rios⁴² ,
589 M. Santimaria²⁴ , L. Santoro¹ , E. Santovetti³² , D. Saranin³⁹ , G. Sarpis⁵⁴ ,
590 M. Sarpis⁷² , A. Sarti³¹ , C. Satriano^{31,u} , A. Satta³² , M. Saur⁵ , D. Savrina³⁹ ,
591 H. Sazak¹⁰ , L.G. Scantlebury Smead⁵⁹ , A. Scarabotto¹⁴ , S. Schael¹⁵ , S. Scherl⁵⁶ , A.
592 M. Schertz⁷³ , M. Schiller⁵⁵ , H. Schindler⁴⁴ , M. Schmelling¹⁷ , B. Schmidt⁴⁴ ,
593 S. Schmitt¹⁵ , O. Schneider⁴⁵ , A. Schopper⁴⁴ , N. Schulte¹⁶ , S. Schulte⁴⁵ ,
594 M.H. Schune¹² , R. Schwemmer⁴⁴ , G. Schwering¹⁵ , B. Sciascia²⁴ , A. Sciucati⁴⁴ ,
595 S. Sellam⁴² , A. Semennikov³⁹ , M. Senghi Soares³⁴ , A. Sergi^{25,n} , N. Serra^{46,44} ,
596 L. Sestini²⁹ , A. Seuthe¹⁶ , Y. Shang⁵ , D.M. Shangase⁷⁹ , M. Shapkin³⁹ ,
597 I. Shchemerov³⁹ , L. Shchutka⁴⁵ , T. Shears⁵⁶ , L. Shekhtman³⁹ , Z. Shen⁵ ,
598 S. Sheng^{4,6} , V. Shevchenko³⁹ , B. Shi⁶ , E.B. Shields^{27,p} , Y. Shimizu¹² ,
599 E. Shmanin³⁹ , R. Shorkin³⁹ , J.D. Shupperd⁶⁴ , B.G. Siddi^{22,l} , R. Silva Coutinho⁶⁴ ,
600 G. Simi²⁹ , S. Simone^{20,i} , M. Singla⁶⁵ , N. Skidmore⁵⁸ , R. Skuza¹⁸ ,
601 T. Skwarnicki⁶⁴ , M.W. Slater⁴⁹ , J.C. Smallwood⁵⁹ , J.G. Smeaton⁵¹ , E. Smith⁶⁰ ,
602 K. Smith⁶³ , M. Smith⁵⁷ , A. Snoch³³ , L. Soares Lavra⁵⁴ , M.D. Sokoloff⁶¹ ,
603 F.J.P. Soler⁵⁵ , A. Solomin^{39,50} , A. Solovev³⁹ , I. Solovyev³⁹ , R. Song⁶⁵ , Y. Song⁴⁵ ,
604 Y. Song³ , Y. S. Song⁵ , F.L. Souza De Almeida² , B. Souza De Paula² ,
605 E. Spadaro Norella^{26,o} , E. Spedicato²¹ , J.G. Speer¹⁶ , E. Spiridenkov³⁹ , P. Spradlin⁵⁵ ,
606 V. Sriskaran⁴⁴ , F. Stagni⁴⁴ , M. Stahl⁴⁴ , S. Stahl⁴⁴ , S. Stanislaus⁵⁹ , E.N. Stein⁴⁴ ,
607 O. Steinkamp⁴⁶ , O. Stenyakin³⁹ , H. Stevens¹⁶ , D. Strekalina³⁹ , Y. Su⁶ , F. Suljik⁵⁹ ,
608 J. Sun²⁸ , L. Sun⁷⁰ , Y. Sun⁶² , P.N. Swallow⁴⁹ , K. Swientek³⁵ , F. Swystun⁵² ,
609 A. Szabelski³⁷ , T. Szumlak³⁵ , M. Szymanski⁴⁴ , Y. Tan³ , S. Taneja⁵⁸ , M.D. Tat⁵⁹ ,
610 A. Terentev⁴⁶ , F. Terzuoli^{30,w} , F. Teubert⁴⁴ , E. Thomas⁴⁴ , D.J.D. Thompson⁴⁹ ,
611 H. Tilquin⁵⁷ , V. Tisserand¹⁰ , S. T'Jampens⁹ , M. Tobin⁴ , L. Tomassetti^{22,l} ,
612 G. Tonani^{26,o} , X. Tong⁵ , D. Torres Machado¹ , L. Toscano¹⁶ , D.Y. Tou³ ,
613 C. Trippl⁴⁵ , G. Tuci¹⁸ , N. Tuning³³ , L.H. Uecker¹⁸ , A. Ukleja³⁷ ,
614 D.J. Unverzagt¹⁸ , E. Ursov³⁹ , A. Usachov³⁴ , A. Ustyuzhanin³⁹ , U. Uwer¹⁸ ,
615 V. Vagnoni²¹ , A. Valassi⁴⁴ , G. Valenti²¹ , N. Valls Canudas⁴⁰ , M. Van Dijk⁴⁵ ,
616 H. Van Hecke⁶³ , E. van Herwijnen⁵⁷ , C.B. Van Hulse^{42,y} , R. Van Laak⁴⁵ ,
617 M. van Veghel³³ , R. Vazquez Gomez⁴¹ , P. Vazquez Regueiro⁴² , C. Vázquez Sierra⁴² ,
618 S. Vecchi²² , J.J. Velthuis⁵⁰ , M. Veltri^{23,x} , A. Venkateswaran⁴⁵ , M. Vesterinen⁵² ,
619 D. Vieira⁶¹ , M. Vieites Diaz⁴⁴ , X. Vilasis-Cardona⁴⁰ , E. Vilella Figueras⁵⁶ ,

620 A. Villa²¹ , P. Vincent¹⁴ , F.C. Volle¹² , D. vom Bruch¹¹ , V. Vorobyev³⁹,
621 N. Voropaev³⁹ , K. Vos⁷⁶ , C. Vrahas⁵⁴ , J. Walsh³⁰ , E.J. Walton⁶⁵ , G. Wan⁵ ,
622 C. Wang¹⁸ , G. Wang⁷ , J. Wang⁵ , J. Wang⁴ , J. Wang³ , J. Wang⁷⁰ , M. Wang²⁶ ,
623 N. W. Wang⁶ , R. Wang⁵⁰ , X. Wang⁶⁸ , Y. Wang⁷ , Z. Wang⁴⁶ , Z. Wang³ ,
624 Z. Wang⁶ , J.A. Ward^{52,65} , N.K. Watson⁴⁹ , D. Websdale⁵⁷ , Y. Wei⁵ ,
625 B.D.C. Westhenry⁵⁰ , D.J. White⁵⁸ , M. Whitehead⁵⁵ , A.R. Wiederhold⁵² ,
626 D. Wiedner¹⁶ , G. Wilkinson⁵⁹ , M.K. Wilkinson⁶¹ , I. Williams⁵¹, M. Williams⁶⁰ ,
627 M.R.J. Williams⁵⁴ , R. Williams⁵¹ , F.F. Wilson⁵³ , W. Wislicki³⁷ , M. Witek³⁶ ,
628 L. Witola¹⁸ , C.P. Wong⁶³ , G. Wormser¹² , S.A. Wotton⁵¹ , H. Wu⁶⁴ , J. Wu⁷ ,
629 Y. Wu⁵ , K. Wyllie⁴⁴ , S. Xian⁶⁸, Z. Xiang⁴ , Y. Xie⁷ , A. Xu³⁰ , J. Xu⁶ , L. Xu³ ,
630 L. Xu³ , M. Xu⁵² , Z. Xu¹⁰ , Z. Xu⁶ , Z. Xu⁴ , D. Yang³ , S. Yang⁶ , X. Yang⁵ ,
631 Y. Yang^{25,n} , Z. Yang⁵ , Z. Yang⁶² , V. Yeroshenko¹² , H. Yeung⁵⁸ , H. Yin⁷ , C. Y.
632 Yu⁵ , J. Yu⁶⁷ , X. Yuan⁴ , E. Zaffaroni⁴⁵ , M. Zavertyaev¹⁷ , M. Zdybal³⁶ ,
633 M. Zeng³ , C. Zhang⁵ , D. Zhang⁷ , J. Zhang⁶ , L. Zhang³ , S. Zhang⁶⁷ ,
634 S. Zhang⁵ , Y. Zhang⁵ , Y. Zhang⁵⁹, Y. Z. Zhang³ , Y. Zhao¹⁸ , A. Zharkova³⁹ ,
635 A. Zhelezov¹⁸ , X. Z. Zheng³ , Y. Zheng⁶ , T. Zhou⁵ , X. Zhou⁷ , Y. Zhou⁶ ,
636 V. Zhovkovska¹² , L. Z. Zhu⁶ , X. Zhu³ , X. Zhu⁷ , Z. Zhu⁶ , V. Zhukov^{15,39} ,
637 J. Zhuo⁴³ , Q. Zou^{4,6} , S. Zucchelli^{21,j} , D. Zuliani²⁹ , G. Zunica⁵⁸ .

638 ¹ Centro Brasileiro de Pesquisas Físicas (CBPF), Rio de Janeiro, Brazil

639 ² Universidade Federal do Rio de Janeiro (UFRJ), Rio de Janeiro, Brazil

640 ³ Center for High Energy Physics, Tsinghua University, Beijing, China

641 ⁴ Institute Of High Energy Physics (IHEP), Beijing, China

642 ⁵ School of Physics State Key Laboratory of Nuclear Physics and Technology, Peking University, Beijing,
643 China

644 ⁶ University of Chinese Academy of Sciences, Beijing, China

645 ⁷ Institute of Particle Physics, Central China Normal University, Wuhan, Hubei, China

646 ⁸ Consejo Nacional de Rectores (CONARE), San Jose, Costa Rica

647 ⁹ Université Savoie Mont Blanc, CNRS, IN2P3-LAPP, Annecy, France

648 ¹⁰ Université Clermont Auvergne, CNRS/IN2P3, LPC, Clermont-Ferrand, France

649 ¹¹ Aix Marseille Univ, CNRS/IN2P3, CPPM, Marseille, France

650 ¹² Université Paris-Saclay, CNRS/IN2P3, IJCLab, Orsay, France

651 ¹³ Laboratoire Leprince-Ringuet, CNRS/IN2P3, Ecole Polytechnique, Institut Polytechnique de Paris,
652 Palaiseau, France

653 ¹⁴ LPNHE, Sorbonne Université, Paris Diderot Sorbonne Paris Cité, CNRS/IN2P3, Paris, France

654 ¹⁵ I. Physikalisches Institut, RWTH Aachen University, Aachen, Germany

655 ¹⁶ Fakultät Physik, Technische Universität Dortmund, Dortmund, Germany

656 ¹⁷ Max-Planck-Institut für Kernphysik (MPIK), Heidelberg, Germany

657 ¹⁸ Physikalisches Institut, Ruprecht-Karls-Universität Heidelberg, Heidelberg, Germany

658 ¹⁹ School of Physics, University College Dublin, Dublin, Ireland

659 ²⁰ INFN Sezione di Bari, Bari, Italy

660 ²¹ INFN Sezione di Bologna, Bologna, Italy

661 ²² INFN Sezione di Ferrara, Ferrara, Italy

662 ²³ INFN Sezione di Firenze, Firenze, Italy

663 ²⁴ INFN Laboratori Nazionali di Frascati, Frascati, Italy

664 ²⁵ INFN Sezione di Genova, Genova, Italy

665 ²⁶ INFN Sezione di Milano, Milano, Italy

666 ²⁷ INFN Sezione di Milano-Bicocca, Milano, Italy

667 ²⁸ INFN Sezione di Cagliari, Monserrato, Italy

668 ²⁹ Università degli Studi di Padova, Università e INFN, Padova, Padova, Italy

669 ³⁰ INFN Sezione di Pisa, Pisa, Italy

670 ³¹ INFN Sezione di Roma La Sapienza, Roma, Italy

671 ³² INFN Sezione di Roma Tor Vergata, Roma, Italy

672 ³³ Nikhef National Institute for Subatomic Physics, Amsterdam, Netherlands

673 ³⁴ *Nikhef National Institute for Subatomic Physics and VU University Amsterdam, Amsterdam,*
674 *Netherlands*

675 ³⁵ *AGH - University of Science and Technology, Faculty of Physics and Applied Computer Science,*
676 *Kraków, Poland*

677 ³⁶ *Henryk Niewodniczanski Institute of Nuclear Physics Polish Academy of Sciences, Kraków, Poland*
678 ³⁷ *National Center for Nuclear Research (NCBJ), Warsaw, Poland*

679 ³⁸ *Horia Hulubei National Institute of Physics and Nuclear Engineering, Bucharest-Magurele, Romania*
680 ³⁹ *Affiliated with an institute covered by a cooperation agreement with CERN*

681 ⁴⁰ *DS4DS, La Salle, Universitat Ramon Llull, Barcelona, Spain*

682 ⁴¹ *ICCUB, Universitat de Barcelona, Barcelona, Spain*

683 ⁴² *Instituto Galego de Física de Altas Enerxías (IGFAE), Universidade de Santiago de Compostela,*
684 *Santiago de Compostela, Spain*

685 ⁴³ *Instituto de Física Corpuscular, Centro Mixto Universidad de Valencia - CSIC, Valencia, Spain*

686 ⁴⁴ *European Organization for Nuclear Research (CERN), Geneva, Switzerland*

687 ⁴⁵ *Institute of Physics, Ecole Polytechnique Fédérale de Lausanne (EPFL), Lausanne, Switzerland*

688 ⁴⁶ *Physik-Institut, Universität Zürich, Zürich, Switzerland*

689 ⁴⁷ *NSC Kharkiv Institute of Physics and Technology (NSC KIPT), Kharkiv, Ukraine*

690 ⁴⁸ *Institute for Nuclear Research of the National Academy of Sciences (KINR), Kyiv, Ukraine*

691 ⁴⁹ *University of Birmingham, Birmingham, United Kingdom*

692 ⁵⁰ *H.H. Wills Physics Laboratory, University of Bristol, Bristol, United Kingdom*

693 ⁵¹ *Cavendish Laboratory, University of Cambridge, Cambridge, United Kingdom*

694 ⁵² *Department of Physics, University of Warwick, Coventry, United Kingdom*

695 ⁵³ *STFC Rutherford Appleton Laboratory, Didcot, United Kingdom*

696 ⁵⁴ *School of Physics and Astronomy, University of Edinburgh, Edinburgh, United Kingdom*

697 ⁵⁵ *School of Physics and Astronomy, University of Glasgow, Glasgow, United Kingdom*

698 ⁵⁶ *Oliver Lodge Laboratory, University of Liverpool, Liverpool, United Kingdom*

699 ⁵⁷ *Imperial College London, London, United Kingdom*

700 ⁵⁸ *Department of Physics and Astronomy, University of Manchester, Manchester, United Kingdom*

701 ⁵⁹ *Department of Physics, University of Oxford, Oxford, United Kingdom*

702 ⁶⁰ *Massachusetts Institute of Technology, Cambridge, MA, United States*

703 ⁶¹ *University of Cincinnati, Cincinnati, OH, United States*

704 ⁶² *University of Maryland, College Park, MD, United States*

705 ⁶³ *Los Alamos National Laboratory (LANL), Los Alamos, NM, United States*

706 ⁶⁴ *Syracuse University, Syracuse, NY, United States*

707 ⁶⁵ *School of Physics and Astronomy, Monash University, Melbourne, Australia, associated to ⁵²*

708 ⁶⁶ *Pontifícia Universidade Católica do Rio de Janeiro (PUC-Rio), Rio de Janeiro, Brazil, associated to ²*

709 ⁶⁷ *School of Physics and Electronics, Hunan University, Changsha City, China, associated to ⁷*

710 ⁶⁸ *Guangdong Provincial Key Laboratory of Nuclear Science, Guangdong-Hong Kong Joint Laboratory of*
711 *Quantum Matter, Institute of Quantum Matter, South China Normal University, Guangzhou, China,*
712 *associated to ³*

713 ⁶⁹ *Lanzhou University, Lanzhou, China, associated to ⁴*

714 ⁷⁰ *School of Physics and Technology, Wuhan University, Wuhan, China, associated to ³*

715 ⁷¹ *Departamento de Física, Universidad Nacional de Colombia, Bogota, Colombia, associated to ¹⁴*

716 ⁷² *Universität Bonn - Helmholtz-Institut für Strahlen und Kernphysik, Bonn, Germany, associated to ¹⁸*

717 ⁷³ *Eotvos Lorand University, Budapest, Hungary, associated to ⁴⁴*

718 ⁷⁴ *INFN Sezione di Perugia, Perugia, Italy, associated to ²²*

719 ⁷⁵ *Van Swinderen Institute, University of Groningen, Groningen, Netherlands, associated to ³³*

720 ⁷⁶ *Universiteit Maastricht, Maastricht, Netherlands, associated to ³³*

721 ⁷⁷ *Tadeusz Kosciuszko Cracow University of Technology, Cracow, Poland, associated to ³⁶*

722 ⁷⁸ *Department of Physics and Astronomy, Uppsala University, Uppsala, Sweden, associated to ⁵⁵*

723 ⁷⁹ *University of Michigan, Ann Arbor, MI, United States, associated to ⁶⁴*

724 ⁸⁰ *Departement de Physique Nucleaire (SPhN), Gif-Sur-Yvette, France*

725 ^a *Universidade de Brasília, Brasília, Brazil*

726 ^b *Centro Federal de Educação Tecnológica Celso Suckow da Fonseca, Rio De Janeiro, Brazil*

727 ^c *Universidade Federal do Triângulo Mineiro (UFTM), Uberaba-MG, Brazil*

728 ^d *Central South U., Changsha, China*

- 729 ^e Hangzhou Institute for Advanced Study, UCAS, Hangzhou, China
730 ^f LIP6, Sorbonne Universite, Paris, France
731 ^g Excellence Cluster ORIGINS, Munich, Germany
732 ^h Universidad Nacional Autónoma de Honduras, Tegucigalpa, Honduras
733 ⁱ Università di Bari, Bari, Italy
734 ^j Università di Bologna, Bologna, Italy
735 ^k Università di Cagliari, Cagliari, Italy
736 ^l Università di Ferrara, Ferrara, Italy
737 ^m Università di Firenze, Firenze, Italy
738 ⁿ Università di Genova, Genova, Italy
739 ^o Università degli Studi di Milano, Milano, Italy
740 ^p Università di Milano Bicocca, Milano, Italy
741 ^q Università di Padova, Padova, Italy
742 ^r Università di Perugia, Perugia, Italy
743 ^s Scuola Normale Superiore, Pisa, Italy
744 ^t Università di Pisa, Pisa, Italy
745 ^u Università della Basilicata, Potenza, Italy
746 ^v Università di Roma Tor Vergata, Roma, Italy
747 ^w Università di Siena, Siena, Italy
748 ^x Università di Urbino, Urbino, Italy
749 ^y Universidad de Alcalá, Alcalá de Henares , Spain
750 ^z Universidade da Coruña, Coruña, Spain
751 [†] Deceased